CHALMERS
UNIVERSITY OF TECHNOLOGY

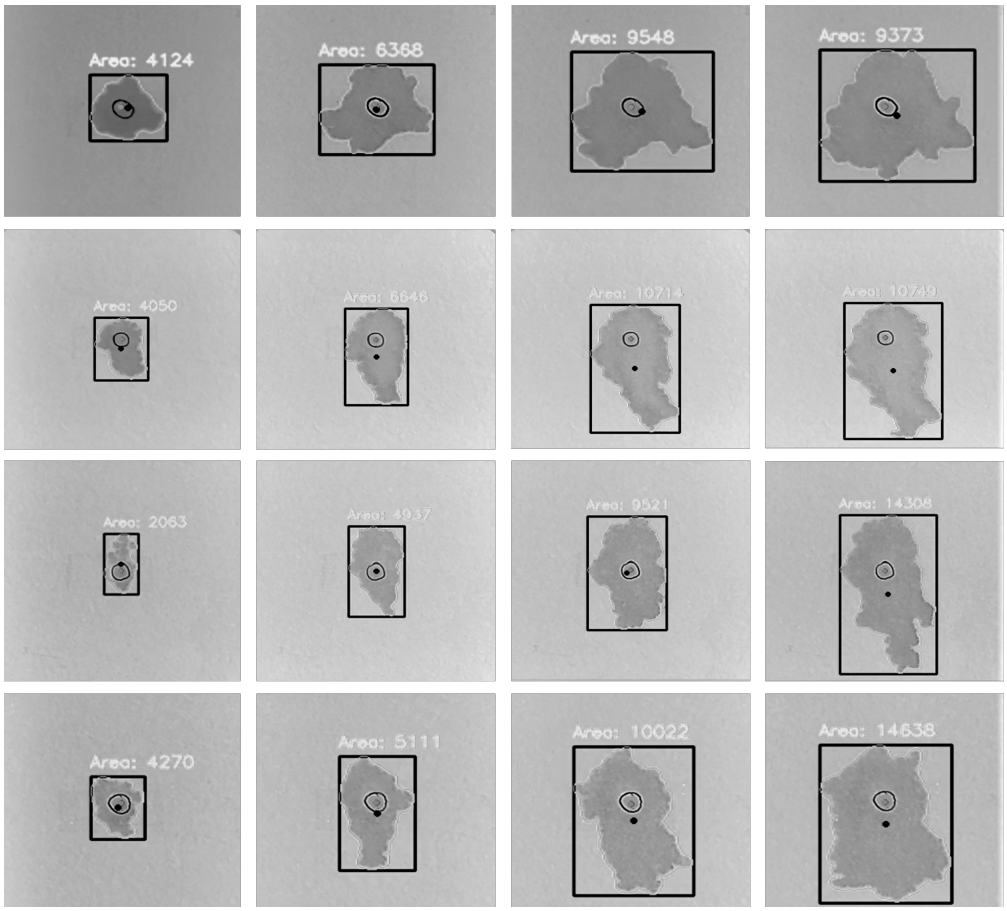

Optimizing the composition of simulated wound fluid to mimic the physico-chemical properties of chronic wound exudate

Master's thesis in Materials Chemistry

IDA JOHANSSON

DEPARTMENT OF CHEMISTRY AND CHEMICAL ENGINEERING
CHALMERS UNIVERSITY OF TECHNOLOGY
Gothenburg, Sweden 2023
www.chalmers.se

Master's thesis 2023

Optimizing the composition of simulated wound fluid to mimic the physico-chemical properties of chronic wound exudate

IDA JOHANSSON

CHALMERS
UNIVERSITY OF TECHNOLOGY

Department of Chemistry and Chemical Engineering
Division of Applied Chemistry
Chalmers University of Technology
Gothenburg, Sweden 2023

Optimizing the composition of simulated wound fluid to mimic the physico-chemical properties of chronic wound exudate
IDA JOHANSSON

Supervisors:
Marina Craig, Mölnlycke Health Care AB
Anna Svensby, Mölnlycke Health Care AB
Romain Bordes, Chalmers University of Technology

Examiner:
Lars Evenäs, Chalmers University of Technology

Master's Thesis 2023
Department of Chemistry and Chemical Engineering
Division of Applied Chemistry
Chalmers University of Technology
SE-412 96 Gothenburg
Telephone +46 31 772 1000

Gothenburg, Sweden 2023

Optimizing the composition of simulated wound fluid to mimic the physico-chemical properties of chronic wound exudate

IDA JOHANSSON
Department of Chemistry and Chemical Engineering
Chalmers University of Technology

Abstract

Chronic wounds pose a significant global health challenge, affecting millions of individuals worldwide. Effective wound management necessitates the use of appropriate wound dressings that provides an optimal environment for wound healing. To accurately evaluate and test wound dressings, it is crucial to employ a test fluid that closely mimics the properties of chronic wound exudate.

This study focused on the formulation and characterisation of a simulated wound fluid used for in vitro testing of wound dressings by optimising the composition of an existing simulated wound fluid (SWF A) and compared important physico-chemical parameters of the test liquid to a serum containing solution (SCS) as the reference solution. Prior studies had shown that the spreading patterns of SCS and SWF A differed, as SCS was forced towards the bottom border of the dressing material by gravitational forces, while SWF A spread more uniformely and did not reach the bottom border of the dressing.

This study showed that the spreading behavior of the fluids depends on both capillary action and aggregation of the fluid proteins in the dressing material. A test fluid (SWF B) that mimics SCS in clinically relevant studies was achieved by optimising the composition of SWF A through altering the BSA content and addition of surfactant. Although SWF B does have the same protein content as SCS, further studies are needed to elucidate the effect of the detailed compositon on the properties and behavior of the test fluid. SWF B, however, mimicked the spreading behavior of SCS well enough to be a contestant for a new standardised test fluid that mimics the physico-chemical properties and spreading behavior of real chronic wound exudate.

Keywords: chronic wounds, wound care, wound exudate, test fluids, simulated wound fluid (SWF), spreading behavior, surface tension, capillary action, protein aggregation, serum albumin

Acknowledgements

First and foremost, I would like to thank Mölnlycke Health Care AB for extending the opportunity to perform my master's thesis at the company. The greatest thanks to my supervisors, Marina Craig, Anna Svensby, and Romain Bordes, for their guidance, support, and invaluable insights. Their expertise and guidance have been vital in shaping this study. I would also like to thank my examinor, Lars Evenäs, for taking on and supporting me during this thesis project.

A special thanks goes out to Jenny Perez-Holmberg, Lina Andreasson, and other team members at Mölnlycke Health Care, for their aid in this study. Their contributions and enthusiasm have greatly enriched this project.

Last but not least, I would also like to acknowledge the employees and students at both MHC and the department of applied chemistry at Chalmers, who have contributed to a warm and open atmosphere for me to work in.

Ida Johansson, Gothenburg, December 2023

List of Acronyms

Below is the list of acronyms that have been used throughout this thesis listed in alphabetical order:

AG	Alkyl Glucoside
BSA	Bovine Serum Albumin
CMC	Critical Micelle Concentration
MHC	Mölnlycke Health Care
MMPs	Metalloproteinases
pI	Isoelectric Point
PU	Polyurethane
ROI	Region of Interest
SCS	Serum Containing Solution
SDS-PAGE	Sodium Dodecyl Sulfate Polyacrylamide Gel Electrophoresis
SEM	Scanning Electron Microscopy
SWF	Simulated Wound Fluid
TIMPs	Tissue Inhibitors of Metalloproteinases

Nomenclature

Below is the nomenclature of indices and parameters that have been used throughout this thesis.

Indices

$_{SV}$, $_{SL}$, $_{LV}$	Indices for interfacial tensions. SV stand for solid-vapor, SL for solid liquid and LV for liquid-vapor interfaces.

Parameters

γ	Interfacial tension
θ	Contact angle

Contents

List of Figures

List of Tables

1
Introduction

Chronic wounds, such as diabetic foot ulcers and pressure ulcers, pose a significant global health challenge, affecting millions of individuals worldwide. These wounds often result from underlying medical conditions such as diabetes, cardiovascular disease, and immobility. If left untreated, chronic wounds can lead to severe morbidity, mortality and substantial economic burden on healthcare systems and society at large. [1, 2] Effective wound management necessitates the use of appropriate wound dressings that provides an optimal environment for wound healing. To accurately develop, evaluate and test new wound dressings, it is crucial to employ a test fluid that closely mimics the properties of chronic wound exudate.

The current European standard for wound care product testing, Test solution A [3], consists of sodium chloride and calcium chloride to achieve an ionic concentration comparable to that of wound exudate. However, wound exudate is a complex, protein-rich solution with variable and dynamic composition, potentially interacting differently with wound dressings compared to solution A. Consequently, there is a need for a standardised test fluid that more accurately replicates wound exudate.

Mölnlycke Health Care (MHC) previously developed a serum-containing solution (SCS) consisting of 50% horse serum and 50% solution A, since the protein concentration of wound exudate has been determined to be around half of the protein concentration in serum, and the electrolyte concentration is considered to be equivalent to serum. [4] However, the use of horse serum presents limitations due to potential compositional variations between different batches. In response, MHC developed a simulated wound fluid (SWF A) as a synthetic substitute, standardising the test fluid by replacing the total protein content with bovine serum albumin (BSA) as the sole protein source while maintaining the ionic strength through salts and buffers.

While the physico-chemical properties such as ionic strength of SWF A and SCS are similar, discrepancies have been observed in material interactions with wound dressings during clinically relevant test evaluations. Specifically, SCS mimics the spreading behavior of real wound exudate where gravitational effects causes a spreading pattern which forces the fluid towards the bottom border of the dressing, whereas SWF A does not exhibit the same behavior. Hypotheses suggest that the higher surface tension of SWF A leads to greater capillary action, counteracting gravitational effects and influencing the spreading pattern. [5] Another hypothesis proposes that proteins in SWF A aggregate more within the wound dressing material, creating a barrier that prevents fluid from flowing with gravity in the material.

The objective of this thesis work is to formulate a standardised test fluid that better represents the material interactions observed with real wound exudate by optimising the composition of SWF A and characterising its physico-chemical properties compared to SCS as the reference solution. Success in this endeavor could establish the optimised test fluid as the standard at MHC and potentially become a new European standard for wound care product testing.

1.1 Scope and aim

In the wound care industry there is currently no standardised test fluid that imitates real wound exudate. The current European standard (Test Solution A) does not sufficiently replicate real wound exudate, while the serum containing solution (SCS) developed by MHC lacks standardisation due to batch variations. The aim of this thesis work is to formulate and characterise a standardised simulated wound fluid for *in vitro* testing of wound dressings by optimising the composition of SWF A. The study will compare essential physico-chemical parameters of test fluids to SCS as the reference solution. The specific objectives of the study are as follow:

- Formulation of a synthetic substitute for SCS to by optimising the composition of SWF A to standardise the test fluid.
- Characterisation of formulated fluids using appropriate analytical methods.
- Investigation of the differences in material interactions between the formulated fluids.
- Validation of the optimised fluid by studying its spreading pattern in a wound dressing material using a clinically relevant wound model for chronic leg ulcers.

By addressing these questions, this study will contribute to the development of more accurate and reliable *in vitro* testing of wound care products. Overall, this study aims to contribute to the improvement of wound care testing methodologies by developing a standardised test fluid that better reflects the behavior and interactions observed with real wound exudate. By achieving this goal, the study has the potential to enhance the evaluation and performance assessment of wound dressings, leading to advancements in the treatment of chronic wounds and ultimately improving patient outcomes.

1.2 Limitations

The study focuses on optimising the simulated wound fluid used for wound dressing testing and will not cover the development or testing of new wound dressings themselves. The emphasis is on formulating simulated wound fluids to mimic real wound exudate in terms of physico-chemical properties and fluid-material interactions. However, the study will not consider the biological and physiological properties or impacts of wound exudate. Additionally, the reformulations of the simulated wound fluid will be kept as simple and cost-effective as possible with regards to

potential additives.

2

Theoretical background

2.1 The wound healing process

The wound healing process is a complex series of events that involves four phases; haemostasis, inflammation, proliferation, and remodelling. These phases work together to facilitate wound closure and restoration of the epithelial skin layer. [6, 7]

The first phase, haemostasis, occurs immediately after tissue injury and can last for two days. It involves vasoconstriction and the release of clotting factors to form blood clots, which stop bleeding and initiate healing. Haemostasis also triggers the inflammatory process. [7, 8]

The inflammatory phase begins shortly after the injury and typically lasts up to seven days in acute wounds and even longer in chronic wounds. It involves the dilation of blood vessels to allow the influx of inflammatory cells and chemicals to the wound site. This phase serves to clear the wound of damaged cells, pathogens, and other bacteria, while preparing the wound bed for new tissue growth. However, the very cells and chemicals associated with the inflammatory phase also elicit typical inflammation symptoms such as swelling, heat, pain and redness. [8, 9]

The proliferation phase is characterised by the formation of granulation tissue, angiogenesis (the formation of blood vessels), wound contraction and epithelialisation (regrowth of skin tissue). It typically lasts for four days to up to three weeks or more. During this phase, new tissue is built, and the wound contracts as myofibroblasts pull the wound edges together. Epithelialisation occurs when epithelial cells resurface the wound area and is promoted by maintaining a moist and hydrated wound environment. [8]

Remodelling, also known as maturation, is the final phase of wound healing and may occur over the span of months or even years. During this phase, tissue fibers are rearranged into a more organised structure, enhancing the tensile strength and elasticity of the healed skin. However, the healed skin typically loses about 20% of its strength and elasticity compared to uninjured skin. This phase can take months or years, depending on the wound severity, location, and treatment methods. [10]

2.1.1 Chronic wounds

Chronic wounds, also known as non-healing wounds, refer to wounds that fail to achieve complete closure within the expected time frame of about 4 to 6 weeks. [6] These wounds are often the result of disruptions in one or more phases of the wound healing process. [11]

Chronic wounds are often associated with patient, wound and/or environmental factors, or a combination of these. Patient-related factors may include underlying conditions such as diabetes, obesity, ischaemia, auto-immune conditions, or malnutrition. Wound-related factors may involve issues such as bacterial and fungal infections, excessive oedema, or inadequate management of wound exudate. Environmental factors, including humidity, desiccation, and lifestyle choices such as smoking or psychological stress, can also influence wound healing. [6]

Studies have demonstrated significant biochemical differences between healing and non-healing wounds. Non-healing wounds are characterised by a prolonged and heightened inflammatory phase, leading to increased exudate production, elevated wound and peri-wound temperature, as well as alkalinity in the wound environment. This alkaline environment disrupts the pH-balance, which normally ranges between 4 and 6 in healthy skin, and instead, it can range from 7.15 to 8.9 in chronic wounds. The altered pH affects the solubility, activity, and physical properties of tissue components such as proteins. The pro-inflammatory wound environment can cause tissue damage and degradation of essential molecules, perpetuating inflammation and hindering the constructive processes necessary for wound healing. Consequently, a cycle of non-healing may ensure, which may persist indefinitely. [6]

Furthermore, chronic wounds provide an optimal environment for bacterial growth due to the elevated pH levels and availability of nutrients from damaged tissue. Bacterial presence can further exacerbate wound conditions as bacterial toxins and additional proteases are released, thus further impeding the healing process. Ultimately, bacteria intensify the pro-inflammatory environment, leading to increased inflammation in the wound. [6]

2.2 Wound exudate

Wound exudate, also known as wound fluid, is produced during the inflammation and proliferation phases of the wound healing process. It is an essential part of the body's inflammatory response to injury. The characteristics of wound exudate, including pH, composition, and temperature, play important roles in wound healing and can serve as potential biomarkers to indicate the progress of the healing process. [12, 13] Two primary functions of wound exudate are to provide essential nutrients for epithelial cells and to maintain a moist wound environment. [14, 15] The exudate volume can vary depending on the stage of wound healing, size of the wound, its origin, and location on the body. [11, 14] In a healing wound, the exudate volume typically decreases over time. However, in non-healing wounds, excessive ex-

udate production may continue due to ongoing inflammation. While a moist wound environment is crucial for optimal healing, excessively wet or dry conditions can negatively impact the healing process. [15]

A study conducted by Trengove et al. (1996) [4] examined the composition of wound exudate from eight patients with chronic leg ulcers in phases of healing and non-healing. Exudate was found to have a high protein content and a composition similar to that of human serum, with similar levels of inorganic electrolytes and approximately half the protein content of serum. [4] The composition of wound exudate is complex and dynamic, comprising water, electrolytes, proteins, enzymes, cells, and other bioactive molecules that are crucial in the wound healing process. [16] Water is the main component of wound exudate, providing the basic medium for the dissolution and transport of other components. Electrolytes, including sodium, potassium, calcium, and magnesium salts, are important for maintaining the ionic balance and osmolality of exudate and contribute to various physiological processes, such as cell signaling, enzyme activities, and tissue repair. Proteins, such as albumin, fibrinogen, and globulins, are abundant in wound exudate and are involved in inflammation, immune response, cell proliferation and tissue remodeling. Enzymes, such as matrix metalloproteinases (MMPs) and tissue inhibitors of metalloproteinases (TIMPs) are important in the degradation and remodeling of extracellular matrix during wound healing. Cells, such as neutrophils, macrophages, fibroblasts, and epithelial cells, are present in wound exudate and have essential functions in the inflammatory and proliferative phases of wound healing. Bioactive molecules, such as cytokines, growth factors, and signaling molecules, are involved in cell signaling, immune response, and tissue repair. [14, 17]

Differences have been observed between the composition of acute wound fluid and chronic wound fluid. Acute wound fluid has been shown to promote wound healing, while chronic wound fluid was found to inhibit epithelialisation. [11, 14] The study by Trengove et al. (1996) [4] compared the composition of wound exudate during the healing versus the non-healing phase. Table (2.1) displays the results, which showed that the total protein content, as well as the albumin content, decreased from the healing to the non-healing phase, while all other components remained more or less the same.

Furthermore, chronic wound exudate may be detrimental to healing as it is more likely to contain bacteria, dead white blood cells, higher levels of inflammatory mediators, and protein-digesting enzymes. [15] It can also be more corrosive than acute wound fluid, potentially causing skin irritation and allergic reactions in the surrounding skin. [16, 18]

Table 2.1: Comparison of total protein and albumin content of wound exudate from eight patients with chronic leg ulcers in healing and non-healing phase. Data is retrieved from Trengove et al. (1996). [4]

Component	Healing		Non-healing	
	Median	Range	Median	Range
Total protein [g/L]	41	36-51	34	26-46
Albumin [g/L]	23	18-28	19	14-24

2.3 Simulated wound fluids (SWFs)

Simulated wound fluids (SWFs) are artificial substitutes for real wound exudate and are used in laboratory and research settings to study wound healing processes, test medical devices, and evaluate the efficacy of various wound care products and treatments. The use of SWFs enables controlled and reproducible experimental conditions, while minimising ethical concerns and variability associated with human or animal studies. The composition of SWFs may vary depending on the specific research objectives and requirements of the study. However, it typically aims to replicate the key characteristics of real wound exudate. [6]

2.3.1 Solution A

According to European standards (EN 13726-1:2002) for primary wound dressing test methods, the current standard test fluid is "Test solution A", which is an ionic solution consisting of sodium chloride and calcium chloride that imitates the ion concentration of human serum or wound exudate. [3]

However, real wound exudate has a more complex composition (with proteins being a key component), meaning that wound exudate exhibit different properties and interact differently with wound dressings compared to solution A. Hence, solution A does not accurately represent the fluid-material interactions of real wound fluid and wound dressings.

2.3.2 Serum containing solution (SCS)

To better simulate real wound exudate, a serum-containing solution (SCS) was developed by MHC. SCS is composed of 50% horse serum and 50% solution A. This formulation was based on the study performed by Trengove et al. (1996), which demonstrated that the protein concentration in wound exudate is half that of serum, while the electrolyte concentration is equivalent to that of serum. [4] However, the composition of horse serum may vary between different batches which makes it difficult to standardise SCS as a test fluid. Nonetheless, SCS sufficiently mimics real wound exudate and is used as the reference solution in this study.

The spreading behavior of SCS in wound dressing material has been previously studied in a clinically relevant simulated wound model for chronic leg ulcers. Figure 2.1

displays the spreading pattern of SCS, which can be observed to spread vertically and reach the bottom border of the dressing material.

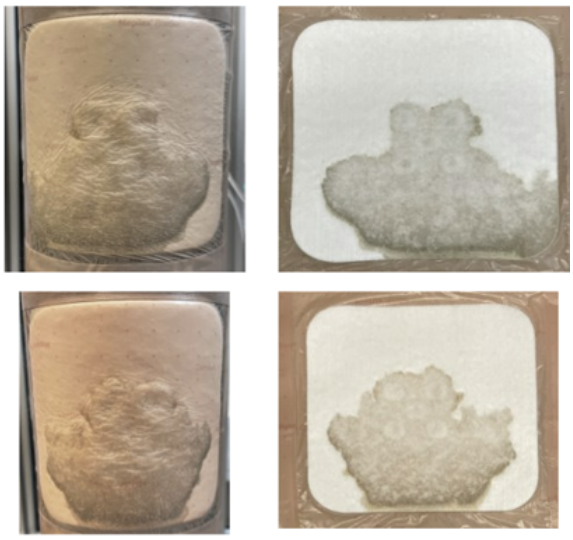

Figure 2.1: Spreading behavior of SCS in wound dressing material

2.3.3 Simulated wound fluid (SWF) A

MHC formulated a simulated wound fluid (SWF A) to achieve a standardised test fluid that better mimics real wound exudate or SCS. The composition of SWF A is based on the composition of non-healing wounds from the study conducted by Trengove et al. (1996). [4] The salt and buffer contents were chosen to achieve an ionic strength and pH similar to wound exudate, while content of bovine serum albumin (BSA) represents the total protein content (34 g/L) of non-healing wounds since albumin is the major protein component (20 g/L) in exudate.

The spreading behavior of SWF A in wound dressing materials has been investigated in a clinically relevant simulated wound model for chronic leg ulcers. Figure 2.2 displays the spreading pattern of SWF A. It can be observed that it spreads more uniformly compared to SCS and does not reaches the bottom border of the dressing material.

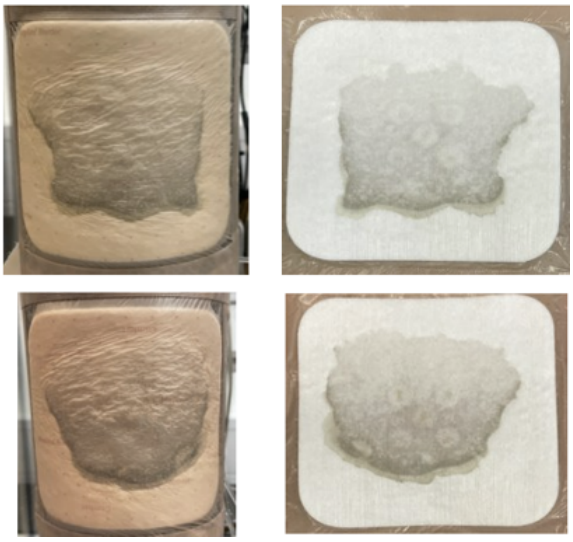

Figure 2.2: Spreading behavior of SWF A in wound dressing material

2.4 Protein solution properties

Protein plays a vital role in wound exudate, making the properties of protein solutions crucial to consider in the context of wound care applications.

Proteins are composed of amino acids covalently linked in a polypeptide chain, with their sequence determining the protein's primary structure. The secondary structure arises from interactions between atoms within the chain, while the tertiary structure involves the configuration, folding, and three-dimensional shape, primarily influenced by interactions between amino acid side chains. Multiple polypeptide chains associating with each other form the quaternary structure, creating a functional protein. [19, 20]

The conformation of proteins relies on environmental factors like pH, temperature, salts, and solvents. Alterations in these factors can denature proteins, leading to a loss of structure and function, resulting in aggregation and precipitation. [21–24]

Amino acids can function as acids or bases, causing proteins to have positive or negative charges depending on the pH. The isoelectric point (pI) represents the pH at which the net charge of the protein is zero. At the isoelectric point, protein stability is reduced, and solubility is at its lowest due to diminished ionic interactions, potentially leading to precipitation and aggregation. [20]

Protein aggregation occurs when proteins associate into larger clusters, influenced by factors such as concentration, temperature, and pH. Aggregation can decrease solubility, impair functionality, and increase immunogenicity. Strategies to mitigate protein aggregation involve controlling solution conditions, such as pH and temperature, and employing excipients for stabilization. [25–27]

The solubility of proteins can vary based on the ionic environment of the solution. Low salt concentrations decrease electrostatic energy between protein molecules, enhancing solubility and preventing aggregation (salting in effect). Conversely, high salt concentrations compete with proteins for water binding, reducing solubility and promoting aggregation (salting out effect). Figure 2.3 illustrates the combined salting in and salting out effects. [28]

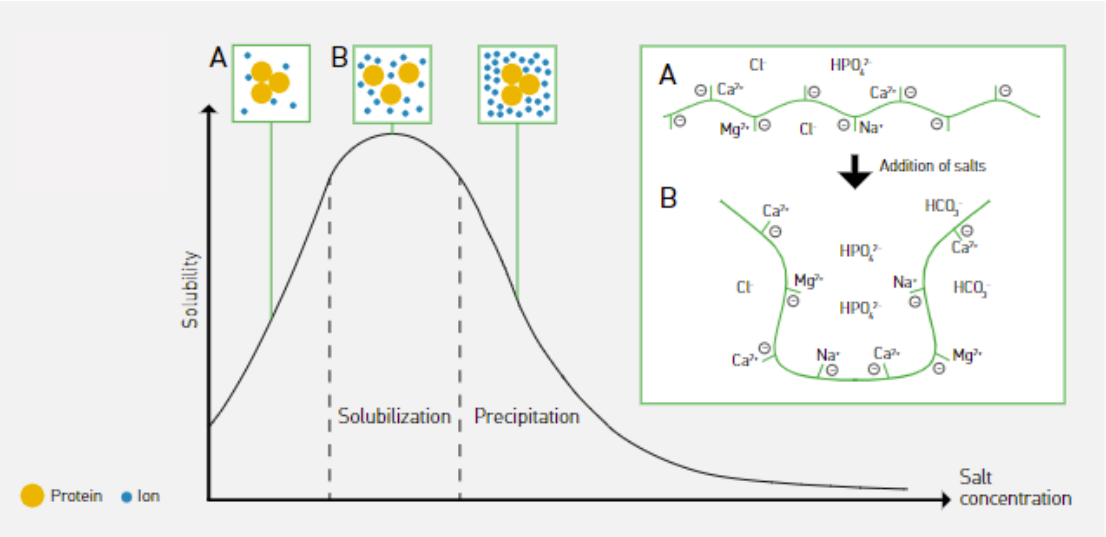

Figure 2.3: The salting in and salting out effect of proteins. [29]

The hydrophobic effect describes the tendency of nonpolar molecules or groups to aggregate in aqueous environments. Hydrophobic regions of proteins interact to minimize contact with water. These interactions' strength depends on temperature, pH, and salt concentration, and they play a crucial role in protein folding, stability, and aggregation. [30]

Temperature significantly impacts protein solubility and stability. High temperatures can cause protein denaturation, resulting in the loss of structure and function, potentially leading to aggregation and precipitation. [20] Furthermore, temperature is also known to effect the viscosity of protein solutions. [31]
The consequence of amphiphilicity of both proteins and surfactants results in that they readily associate through electrostatic, hydrophobic, and Van der Waals interactions, the prominence of which depends on the specific natures of a protein and a surfactant, respectively. These molecular interactions impacts the protein structures and could either promote or prevent denaturation and aggregation. [32]

Some important physical parameters that impact the surfactant-protein interactions include the chemical nature of the surfactant and the surfactant concentration. In this project a nonionic surfactant (alkyl glucoside) is used. Nonionic surfactants tend to have weak molecular interactions with proteins, thus decreasing protein aggregation and increasing protein solubility. Surfactant concentrations above the critical micelle concentration (CMC) may promote protein denaturation and aggregation,

whilst concentrations far below the CMC usually induce protein stabilisation. [32]

2.5 Wound dressings

Proper wound management is essential for promoting healing of chronic wounds. The characteristics of a wound often varies and the selection of a wound dressing must be adapted accordingly. Some important properties of a good wound dressing include its ability to absorb wound exudate, maintain a moist wound environment, minimise skin maceration, allow evaporation, facilitate easy removal, and minimise patient discomfort. [33]

Chronic wounds often exhibit high levels of exudate, which can contribute to infection and delayed healing. Therefore, these wounds require dressings with high absorption and rapid moisture vapour loss to manage the exudate levels effectively. Absorbent dressing materials prevent wound fluid from reentering the wound to protect the periwound skin. Examples of absorbent wound dressings include hydrocolloids, alginates, and foams. [33]

The dressing used by MHC to study and compare the different test fluids mentioned in section (2.3) is a five-layer foam dressing called Mepilex Border Flex (Figure 2.4). The dressing consists of the following layers:

- Safetac wound contact layer, a soft silicone adhesive material that minimises pain during dressing changes by not adhering to the wound directly.
- Absorbent foam layer that rapidly absorbs exudate vertically with minimal lateral spreading.
- Spreading layer, a nonwoven material that improves the effectiveness of the absorption layer and the backing film's vapour release by absorbing and spreading the exudate evenly across its surface.
- Retention layer that consists of cellulose fibers, superabsorbent fibers and binding polymers. It has absorption and retention capacity, and the superabsorbent fibers prevents bacteria from reentering the wound bed.
- Backing film that is highly breathable while also stopping bacteria and viruses from entering.

Figure 2.4: Five layers of Mepilex Border Flex. From bottom-up: 1) Safetac wound contact layer, 2) absorbent foam layer, 3) spreading layer, 4) retention layer, 5) backing film. From [36].

The combined spreading and retention layer, known as an airlaid material, is where the main differences in fluid spreading have been observed. The spreading layer is made of a nonwoven material, whilst the retention layer consists of cellulose fibers, superabsorbent fibers and binding polymers. Both cellulose and superabsorbent fibers exhibit high hydrophilicity, enabling effective water absorption and retention within the dressing. [34, 35]

2.6 Spreading behavior

Absorbent wound dressings are designed to absorb, retain and/or evaporate wound fluid in order to manage excessive moisture, promote a moist wound environment and prevent maceration of the surrounding skin. [37] Fibrous and porous materials, such as those used in this project, are complex and their interactions with fluids varies depending on specific material properties.

Fluid transport involves both liquid and vapour transmission, and can be described as a three step process. The first step is wetting and the rapid diffusion of vapour in the gas phase of the void spaces between fibres, along with the surface tension-driven process of liquid spreading through wicking. The second step is the moisture sorption of the fibers, where vapour is absorbed by the fibers due to their chemical composition and structure. liquid absorption is also facilitated by the molecular interactions between fibers and liquid. This molecular interactions are influenced by

capillary action, which depends on surface tension, pore distribution and pathways. Fiber moisture sorption may last for minutes or hours depending on heat transfer processes. Lastly, the third stage is reached when fluid and heat transfer processes reach an equilibrium. In other words when fluid absorption and desorption in the material is in balance. When this condition is met, the temperature distribution, fluid vapour concentration, fiber fluid content, liquid fraction volume, and evaporation all become constant. This equilibrium also establishes a finite state of the spreading pattern and amount of fluid in the dressing material. [38, 39]

2.6.1 Diffusion

Diffusion is driven by concentration- and vapour pressure gradients. A fluid can diffuse through a porous fibre material either in the void spaces between fibers or along and within the fibres. The former is a fast process whilst the latter is limited by the rate at which the fluid can diffuse into and out of the fibres. [38] Fibers can also absorb fluids due to internal chemical compositions and structures that cause an affinity for each other, such as hydrophilic properties. [39] Superabsorbent fibers, mentioned earlier, are excellent examples of fibers that absorb fluids due to their hydrophilicity. [40]

2.6.2 Wetting

Wetting is a complex process that depends on liquid properties, material characteristics, and environmental conditions. It involves several primary processes: capillary sorption, adhesion, and spreading. Capillary sorption occurs when the liquid comes into contact with the solid material, replacing the solid-vapour interface with a solid-liquid interface. Adhesion refers to the attraction between the solid and the liquid, while spreading refers to the expansion of a liquid over a solid. [41]

These processes depend on interfacial tensions, which represent the interfacial energies between different phases. The interfacial tensions considered are the solid-vapor interface (γ_{SV}), the solid-liquid interface (γ_{SL}), and the liquid-vapor interface (γ_{LV}). [41] Figure 2.5 illustrates the angle at which the liquid, gas, and solid intersect, known as contact angle (θ), which can be used as a quantitative measurement of wetting. At equilibrium, the contact angle and the interfacial tensions can be correlated using Young's equation (Eq.(2.1)).

$$\gamma_{SV} - \gamma_{SL} = \gamma_{LV} \cdot \cos\theta \tag{2.1}$$

A low contact angle indicates hydrophilicity. Conversely, a large contact angle suggest that the material is hydrophobic and does not readily get wet by the liquid. [41] Wound fluid contains large amounts of water, so if the contact angle between the wound fluid and wound dressing is less than 90°, the fluid wets the material, indicating hydrophilicity. On the other hand, if the contact angle is greater than 90 °, the fluid does not wet the material, indicating hydrophobicity. [42]

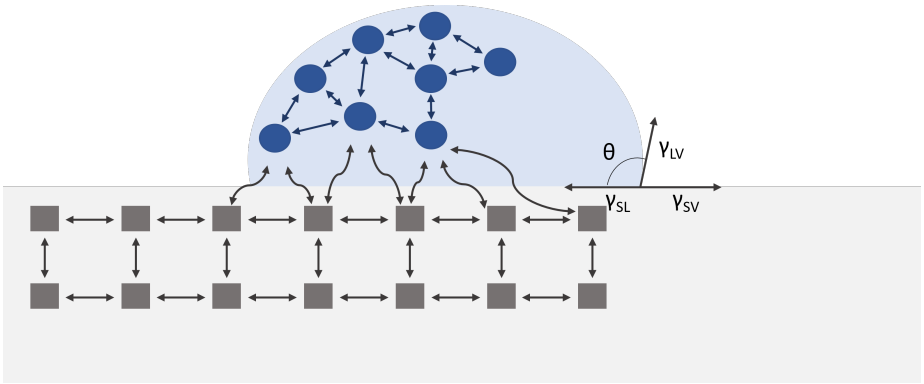

Figure 2.5: Representation of contact angle

2.6.3 Wicking

Wetting is a prerequisite for wicking, since when the liquid wets the solid, the surface energy of the solid is altered by the invading liquid, which causes a negative capillary pressure that drives the liquid into the capillary spaces between the fibers of the solid phase. [43] This capillary action occurs when the adhesive forces between the liquid and the solid is greater than the cohesive forces between the liquid molecules. These forces give rise to interfacial tensions, hence wicking is highly dependent on interfacial tension and contact angles. [44] Furthermore, wicking also depends on the viscosity of the fluid and the size of the capillaries in the wound dressing material. [41]

Wicking occurring perpendicular to the plane of the material, i.e. straight through the thickness of the material, is referred to as transplanar wicking. In wound care, this is the main direction of wicking due to the orientation of wound dressings. Since the thickness of the material is relatively small, the liquid quickly permeates through the material, thus making it more challenging to measure transplanar wicking compared to longitudinal wicking. [41]

Liquid diffusion into the interior of the fibers can cause swelling, which reduces the space between fibers and the size of the capillaries. [41] Apart from complicating the pore structure, fiber swelling also reduces the wet fiber strength and resiliency, which can lead to pore collapse and a decrease in liquid holding capacity. [45] It is important to note that compression applied to the wound dressing can alter the size and structure of the fibers and pores. Furthermore, some fibers themselves may be porous, thus creating secondary capillaries, which adds another layer of complexity the wicking process.

2.6.4 Gravitational forces

Wicking and capillary action works against the force of gravity, however, in wound dressings the fluid may still flow downward in the material due to the pull of gravity. The extent to which gravity affects the liquid flow in wound dressings will depend on various factors, such as the physico-chemical properties of the fluid (e.g., viscosity and surface tension) and the material (e.g., pore size and surface chemistry), as

well as the orientation and positioning of the dressing. These factors collectively determine the balance between capillary action and gravitational forces, influencing the direction and extent of liquid flow within the material.

2.6.5 Retention

Fluid retention in wound dressings refers to the balance between absorption and release of fluid by the material. In other words, it is the equilibrium between fluid flow from the wound and the amount of fluid that is evaporated, or squeezed out by external forces, from the wound dressing. This mass balance is important to ensure that the wound is kept moist, while preventing excessive fluid build-up that can lead to maceration and infection. [38]

2.6.6 Evaporation

Fluid transport is not only dependent on mass transfer, but also heat transfer. The mechanism of which include conduction through the solid material of the fibers, conduction through intervening air, radiation, and convection. The combination of heat and mass transfer induces phase changes such as fluid sorption/desorption and evaporation/condensation. The latter of which depends on temperature and moisture distribution. [39, 46]

By controlling the water evaporation from a wound, the optimal moisture levels can be achieved to promote wound healing and to increase wear-time of the dressing. [47] Evaporation of water and/or other components may concentrate or influence the composition of the wound fluid that remains in the wound and the wound dressing. [15] The concentration of proteins in the fluid may induce protein aggregation and heterogeneity of the protein solution. [48]

3
Methodology

This section outlines the methodology employed for preparing test fluids, analysing their physico-chemical properties, and evaluating their spreading behavior in wound dressing materials. The test fluids were meticulously prepared in a laboratory setting following a standardised protocol. Various measurements, including pH, conductivity, surface tension, viscosity, and contact angle, were performed using established techniques to characterise the test fluids. To assess fluid absorption and spreading in materials, a combination of wicking experiments, a clinically relevant simulated wound model for chronic leg ulcers, scanning electron microscopy (SEM), inclined plane method, and image analysis were utilised. These methodologies collectively contributed to gaining a comprehensive understanding of the composition, properties, and interactions of test fluids with dressing materials.

3.1 Preparation

The preparation of the fluids used in this study is crucial as it influences their properties and behavior in terms of fluid-material interactions. Test fluids for wound care products aim to simulate real wound exudate to varying degrees, depending on the intended use and existing protocols. This section provides a detailed description of the methodology employed for preparing the test fluids mentioned in section (2.3).

3.1.1 Solution A

Solution A, known as the current European standard test liquid, is composed of sodium chloride, calcium chloride, and water. It was prepared by dissolving 8.298 g/L sodium chloride and 0.368 g/L calcium chloride in deionised water. The solution was pre-prepared by MHC and readily available throughout the study.

3.1.2 Serum containing solution (SCS)

SCS aims to replicate the biochemistry of real wound exudate, as discussed in section (2.3.2). It was prepared by mixing 50 wt % horse serum and 50 wt % solution A to achieve the ionic strength and protein content similar to that of real wound exudate. The fast and simple preparation of SCS allows for direct usage without extensive preparation, sterile filtration and storage. However, in this study, SCS was also sterile filtered and compared to non-filtered SCS. These fluids were investigated in regards to surface tension measurements and whether the filtration process removed important components in the fluid.

3.1.3 Simulated wound fluid A (SWF A)

SWF A was designed to provide a standardised test fluid that mimics real wound exudate and/or SCS. Table (3.1) displays the composition of SWF A. The salt and buffer components (excluding calcium chloride, which causes protein precipitation if added before the BSA) were individually weighed and added to approximately 800 mL of deionised water for mixing using a magnetic stirrer. Once all the reagents had completely dissolved, the protein component BSA (freeze dried powder) was weighed and added. Stirring was performed gently to prevent foaming. Complete solvation of the protein took approximately 2-3 hours. After protein solvation, calcium chloride was weighed, dissolved in approximately 100 mL of deionised water, and added to the solution. The the final volume of the test fluid was adjusted to 1 L with deionised water. The final solution was then sterile filtered.

Table 3.1: Composition of SWF A

	Ingredients	[mmol/L]	[g/L]
Salts	Sodium chloride, NaCl	110	6.428
	Calcium chloride, $CaCl \cdot 6H_2O$	2.2	0.323
	Potassium chloride, KCl	2.7	0.199
	Magnesium chloride, $MgCl_2 \cdot 6H_2O$	0.5	0.102
Protein	Bovine Serum Albumin (BSA), fraction V	N/A	34
Buffers	Potassium phosphate monobasic, KH_2PO_4	1.3	0.177
	Sodium bicarbonate, $NaHCO_3$	20	1.68

The original composition of SWF A contained 34 g/L BSA to replace the total protein content in wound exudate. However, wound exudate only contains 20 g/L BSA, with the remaining 14 g/L comprising other proteins. Therefore, SWFs with 34, 20, and 10 g/L were prepared to analyse the impact of protein content on fluid properties.

3.1.4 Sterile filtration

To prevent bacterial growth that could alter the properties of the fluids, the fluids underwent sterile filtration using a 0.2 μm pore size polyethersulfone (PES) membrane suitable for sterile filtration of media and serum. The filtration setup (Figure 3.1) involved connecting a pump (A) to a protection filter (B), which was then attached to a separator flask (C) fixed with a stand (D). A sterile receiver flask (F) was attached to the serum filter (E), which was connected to the separator flask (C). Once the filtration equipment was set up the pump was started, the test fluid was poured into the filter (E) and collected in the sterile receiver flask (F).

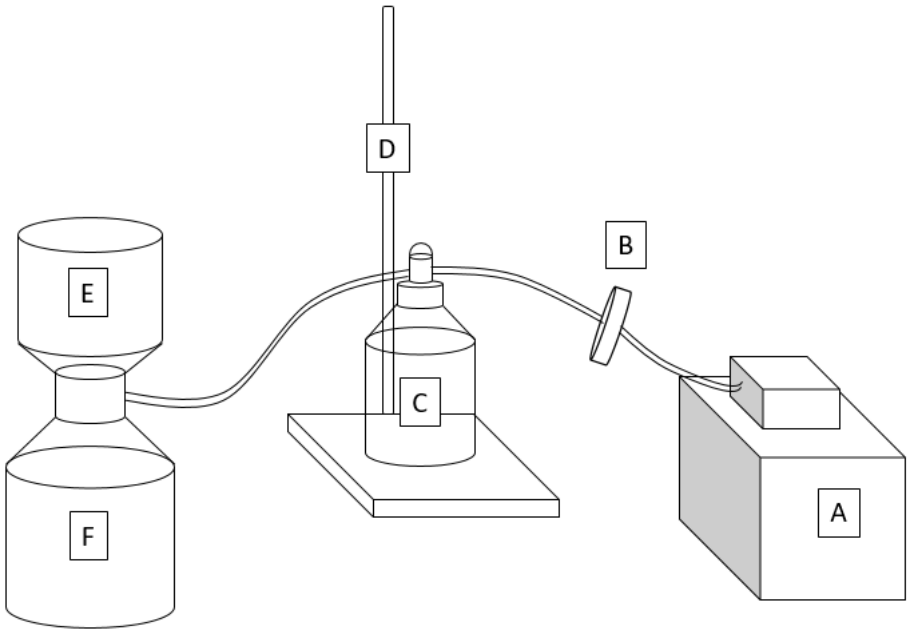

Figure 3.1: Set up of the filtration equipment

3.1.5 Addition of surfactant

In a later stage of the study, surfactant (alkyl glucoside (AG)) was introduced to SWF A and SWF 20 (SWF with 20 g/L BSA) to mimic the surface tension of SCS. Various proportions (weight %) of AG were added to the SWFs until the desired surfactant concentration for achieving the target surface tension was reached. The process involved placing a glass vial on a scale, followed by pipetting the alkyl glucoside into the vial and measuring the weight of the added surfactant. Approximately 10 g of SWF was then added to the vial and weighed. The vial was gently shaken to ensure dissolution of the surfactant solution. Subsequently, surface tension measurements were conducted. Initially, surfactant was added to SWF 20, and the weights and concentrations are provided in Table (3.2). The resulting fluid, designated as SWF B, represented an optimised version of SWF A and was used in subsequent studies. It successfully achieved the desired surface tension by incorporating an appropriate concentration of AG, while also adjusting the BSA content to closely mimic SCS. However, while the BSA content of SWF B was similar to that of SCS, the total protein concentration was 14 g/L less.

Table 3.2: Concentrations of alkyl glucoside in SWF 20

Mass		Concentration [%]
Alkyl glucoside [mg]	SWF 20 [g]	
1.42	10.6959	0.013
2.30	10.0497	0.023
3.81	10.0150	0.038
4.83	9.9933	0.048
11.07	10.0003	0.111
14.49	10.0300	0.144
19.20	10.0058	0.192
30.77	9.9969	0.308
39.04	9.9667	0.392
60.07	10.0187	0.600
100	9.9799	1.002

The surface tension measurements of SWF 20 with added surfactant, narrowed down the concentration range required for establishing a similar surface tension for SWF A (34 g/L BSA) with added surfactant. The weights and concentrations of the surfactant solutions in SWF A are presented in Table (3.3). The resulting fluid, designated as SWF C, represented an optimised version of SWF A and was used in subsequent studies. It successfully achieved the desired surface tension by incorporating an appropriate concentration of AG, while maintaining a total protein content of 34 g/L. However, as for SWF A, the sole protein source in SWF C consisted of BSA and not the full range of serum proteins found in SCS.

Table 3.3: Concentrations of alkyl glucoside in SWF A

Mass		Concentration [%]
Alkyl glucoside [mg]	SWF 20 [g]	
2.5	10.0020	0.025
2.8	10.0095	0.028
4.5	10.0282	0.045
10.4	10.0480	0.104
14.6	10.0802	0.145
20.6	10.0373	0.205

3.2 Physico-chemical properties

This section focuses on investigating the physico-chemical properties of the test fluids. Carefully controlled preparation and standardized measurement techniques were employed to analyse properties such as pH, conductivity, surface tension, viscosity, contact angle, and protein composition. These measurements provided crucial insights into the behavior and interactions of the fluids with wound dressing materials.

3.2.1 pH

pH measurements were conducted to assess the acidity or alkalinity of the test fluids, aiming to mimic the pH of chronic wound exudate. A pH meter was used for quantitative assessment of the hydrogen ion concentration in a solution, determining its pH value. A pH meter typically consists of a reference electrode, a sensor electrode, and a pH meter unit. The reference electrode contains a liquid with a known electric potential, while the sensor electrode is inserted into the test fluid. The potential difference between the electrodes is converted into pH values displayed on a digital screen of the pH meter unit. To ensure accurate measurements, a calibration procedure was conducted. The pH electrode was immersed in standard buffer solutions with known pH values (4, 7, and 10), allowing sufficient time for stabilisation. The pH meter readings were adjusted based on the known pH values until proper calibration was achieved. Prior to pH measurements, the pH electrode was rinsed with distilled water to eliminate any residual contaminants. Subsequently, the electrode was immersed in the sample solution, and the pH reading was allowed to stabilise until a constant reading was obtained and recorded. Multiple measurements were performed for each sample to ensure precision and reproducibility, and the average pH was calculated to minimise measurement errors.

3.2.2 Conductivity

Conductivity measurements were conducted to assess the electrical conductivity of the test fluids, providing insights into the ion concentration of the solution. This ensured that the ionic composition of the test fluids resembled that of real wound exudate. The experiment was performed using a conductivity meter, consisting of a conductivity probe, a temperature sensor, and a meter display unit. The probe, containing electrodes, was immersed in the solution, allowing electric current to pass through it. The probe measured the electrical conductance of the solution, which was converted into a conductivity value that is directly proportional to the ion concentration. Conductivity is temperature dependent, and the temperature sensor compensated for variations ensuring accurate readings. Calibration was performed using a standard solution with a known conductivity value (12.88 mS/cm). Prior to measuring, the probe was rinsed with distilled water to eliminate any residual contaminants. Subsequently, the probe was immersed in the sample solution, and the conductivity reading was allowed to stabilise until a constant reading was obtained and recorded. Multiple measurements were performed for each sample to ensure precision and reproducibility, and the average conductivity was calculated to minimise measurement errors.

3.2.3 Surface tension

Surface tension was measured using the Du Noüy ring method. In this method, a ring, usually made of platinum, is immersed in the test fluid, and the force required to detach the ring from the liquid surface is measured and correlated to the surface tension of the liquid (see Figure 3.2).

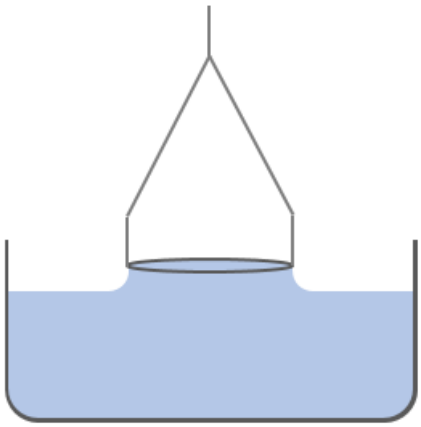

Figure 3.2: Du Noüy ring method

The experimental setup consisted of a ring attached to a thin metal wire connected to a force sensor. Prior to and after testing, the ring was carefully cleaned with a burner to remove any contaminants and ensuring accurate measurements. To calibrate the system, the ring was immersed in a reference liquid with known surface tension, such as Milli-Q water. Careful handling of the fluid samples was employed to prevent any potential contamination that could affect the measurements, and the beaker holding the liquid was properly cleaned. The surface tension measurements were performed for 10-15 minutes per sample to ensure stabilisation. Multiple replicates were conducted for each sample to ensure precision and reliability. The average surface tension was calculated to minimise potential measurement errors.

3.2.4 Viscosity

Viscosity of the fluids was measured using a Brookfield viscometer, which operates based on rotational viscometry. A cylindrical sample chamber was filled with the test fluid, and a spindle connected to a motor was immersed into the fluid. The motor rotated the spindle at a controlled speed, and the torque required to overcome resistance to rotation was measured. The measured torque was directly related to the viscosity of the fluid. Calibration of the viscometer was performed using a reference fluid with known viscosity values, such as water. The sample fluids were prepared in advance and precautions were taken to minimise any potential changes in viscosity due to temperature fluctuations or other environmental factors. Measurements were conducted within a consistent time span of 10 minutes per sample to ensure stabilisation and precision.

3.2.5 Contact angle

The contact angle between a liquid droplet and a solid surface at the point of contact was determined using a contact angle goniometer. A goniometer is an optical instrument that consists of a drop dispenser, a sample stage, a light source to illuminate the droplet, a camera, and software for image analysis. Considering that the materials used in this study are hydrophilic and absorptive, it was deemed more appropriate to select a non-absorbing material. In this study, the Safetac silicone

material used in the wound contact layer of Mepilex border flex (as described in section (2.5)) served as an appropriate substrate, despite its hydrophobic properties.

To measure the contact angle, a droplet of the test fluid was carefully placed onto the substrate using a syringe. An image was captured of the droplet and the contact line where the liquid meets the solid. The lighting and camera settings were optimised to ensure clear visibility. Subsequently, specialised software was utilised to process the captured image and determine the contact angle. To account for any potential variations or uncertainties, multiple measurements were performed for each fluid by placing droplets on different locations of the substrate, and multiple images were taken per droplet.

3.2.6 SDS page electrophoresis

SDS-PAGE (Sodium Dodecyl Sulfate Polyacrylamide Gel Electrophoresis) was used to analyse the protein composition and molecular weight distribution of the test fluids. This technique is widely used in biochemistry and molecular biology to separate proteins based on their molecular weight. SDS-PAGE was primarily employed in this study to assess the differences between SCS (containing the full range of serum proteins), SWF A (containing only BSA), and SWF B and C (containing BSA and surfactant).

The gel used in SDS-PAGE was purchased from Bio-Rad Laboratories, and consisted of a highly cross-linked matrix that acted as a protein sieve. The gel was placed in the gel chamber of an electrophoresis cell, which consisted of a lower buffer chamber and an upper gel chamber. The gel chamber was carefully filled with a tank buffer, such as Tris-glycine or Tris-Tricine, which provided the necessary ionic environment for protein migration during electrophoresis.

The test fluids were mixed with a sample buffer containing SDS (Sodium Dodecyl Sulfate) and a reducing agent, such as 2-mercaptoethanol, to denature and unfold the proteins into linear chains, imparting a uniform negative charge. This denaturation process ensured that the proteins would migrate primarily based on their molecular weight rather than their native structure. The denatured protein samples were heated at an elevated temperature, typically around 95C, for about 5 minutes to ensure complete denaturation. Once denatured, the protein samples were mixed with a loading dye, which contained tracking dyes that aided in visualizing the migration front during electrophoresis. Care was taken to thoroughly mix the protein samples with the loading dye through centrifugation to ensure even distribution and accurate representation of the protein content. The protein samples, along with molecular weight markers of known sizes, were loaded into the wells of the gel using a micropipette. Multiple replicates of each sample were loaded to ensure reproducibility.

Once the samples and markers were loaded, the electrophoresis cell was connected to a power supply, and a voltage of approximately 200 V was applied. An electric current was passed through the gel matrix, causing the negatively charged proteins

to migrate towards the positive electrode. The migration rate was primarily determined by the molecular weight of the proteins, with smaller proteins moving more easily through the pores of the gel and traveling farther, while larger proteins encountered more resistance and migrated shorter distances. The electrophoresis run time was carefully controlled to allow for sufficient migration of the proteins through the gel, ensuring clear separation and visualization of distinct protein bands.

After the electrophoresis was completed, the gel was carefully removed from the electrophoresis cell. It was then immersed in a protein stain solution, Coomassie Brilliant Blue R-250, which bound to the proteins and allowed for their visualization. The gel was incubated in the stain solution for a approximately 40 minutes, ensuring adequate penetration and staining of the proteins. Excess stain was subsequently removed by destaining the gel with a destaining solution, which improved the contrast between protein bands and reduced background staining.

The stained gel was scanned to capture an image of the separated protein bands. Molecular weight markers were used as references to calibrate the gel image and accurately determine the approximate molecular weight of the separated proteins.

3.3 Spreading behavior

This section outlines the methodology employed to study the spreading behavior of test fluids within wound dressing materials. Understanding how fluids distribute within dressings is crucial for assessing their effectiveness in managing wound exudate, and it enables differentiation of test fluids based on the fluid-material interactions. The experimental techniques used included wicking tests, FLUHTE experiments, scanning electron microscopy (SEM), inclined plane testing, and image analysis. These methods provide valuable insights into fluid absorption, material interaction, and quantitative characterisation of spreading patterns, facilitating a comprehensive understanding of fluid behavior within wound dressing materials.

3.3.1 Wicking

Wicking tests were conducted to evaluate the capillary action and absorbency of materials, specifically to assess the wicking behavior of different fluids. Vertical wicking testing, a type of wicking test, was employed to measure the ability of materials to draw liquid vertically and against gravity.

The experimental setup, depicted in Figure 3.3, involved immersing the lower end of a material sample in a beaker containing the test fluid. Through capillary action, the liquid moved upward through the material. After a 5-minute period, the height to which the liquid rose was measured. Additionally, the weight of the material sample was measured before and after liquid immersion to determine the absorbed fluid weight.

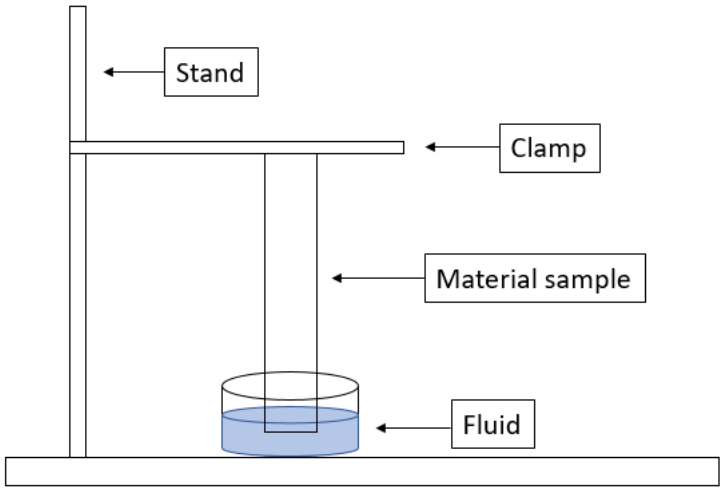

Figure 3.3: Wicking testing set up

Several materials were tested to identify the most suitable material(s) for evaluating wicking behavior. The materials used in this study included polyurethane (PU) foam, airlaid, filter paper, and printer paper. To assess wicking behavior, two liquids with significantly different surface tensions were employed. Water and ethanol, with known surface tensions of approximately 73 and 22 mN/m respectively, were selected to demonstrate contrasting wicking behavior. Once the appropriate material(s) were determined, the evaluation of different test fluids was initiated.

3.3.2 FLUHTE

The spreading behavior of different fluids in the airlaid material (the combined spreading and retention layer of Mepilex border flex) were studied using a clinically relevant simulated wound model for chronic leg ulcers developed by MHC. The experimental setup, known as FLUHTE, aimed to replicate the conditions for exudate management of a wound dressing when applied to a chronic wound.

The product was assembled by attaching a 15x15mm airlaid pad onto an adhesive backing film material. After measuring the weight of the dry product, it was attached to the simulated leg with the product's machine direction oriented vertically. The product was covered by two layers of wadding and a low elastic single-layer bandage was wrapped around the leg to apply pressure, as depicted in Figure 3.4. The test fluid of choice was pumped into the product dressing material under defined conditions, including temperature, pressure, and flow rate. In this study, a temperature of 32°C, a pressure of 40 mmHg, and a flow rate of 1 mL/h were set, with a total test time of 24 hours. Several replicates were conducted to ensure precision and reliability. After the test duration, the weight of the wet product was measured to calculate the amount remaining and evaporated fluid. If further study of the fluid-material interactions was required, the product was dried and analysed using scanning electron microscopy (SEM).

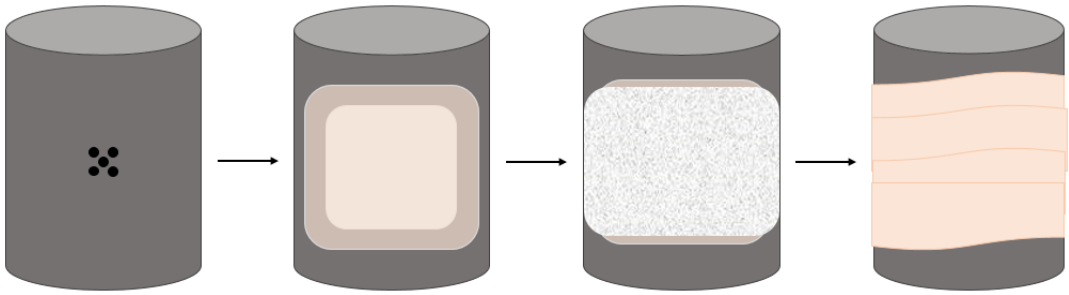

Figure 3.4: Schematic of the FLUHTE method

3.3.3 Scanning electron microscopy (SEM)

SEM, a technique for obtaining high-resolution images of a sample's surface was utilised to study fluid-material interactions observed during the FLUHTE tests. SEM provides information about the morphology, topography, and composition of the material under examination. In this study, SEM was primarily employed to visualise potential protein aggregation and to investigate compositional variations in the regions of the dressing saturated by the fluid.

The principle of SEM involves scanning a focused electron beam across the sample's surface, which generates various signals, including secondary electrons, backscattered electrons, and characteristic X-rays. These signals are detected and used to generate an image of the sample's surface.

During the SEM-analysis, the sample, which was previously subjected to fluid absorption, was prepared for imaging. The dried sample was carefully mounted on a holder and coated with a thin layer of gold through sputtering. The conductive coating helped to minimise charging effects and improve the image quality. Once the sample was prepared, it was placed inside the SEM chamber which subsequently was filled with vacuum. Imaging parameters were set and the electron beam was scanned across the sample's surface to generate the SEM-images.

3.3.4 Inclined plane

The inclined plane method, developed by MHC, was employed to determine the absorption capacity and dispersion ability of materials when subjected to compression and gravity with the addition of a test liquid at a constant flow rate.

As illustrated in Figure 3.5, the inclined plane setup consisted of fixing a specimen with a plexiglass plate on the inclined plane. The distance between the plane and plate was adjusted to apply a predefined pressure of 40 mmHg based on the material thickness, which was determined through thickness measurements performed under the set pressure. A test fluid was then introduced at a constant flow rate into the centre of the specimen material from underneath. The flow rate and test time were adjusted according to predefined conditions. In this study a flow rate of 0.5 mL/h

and a test time of 4 hours were determined to yield the desired results. To ensure precision and reliability, multiple replicates were tested.

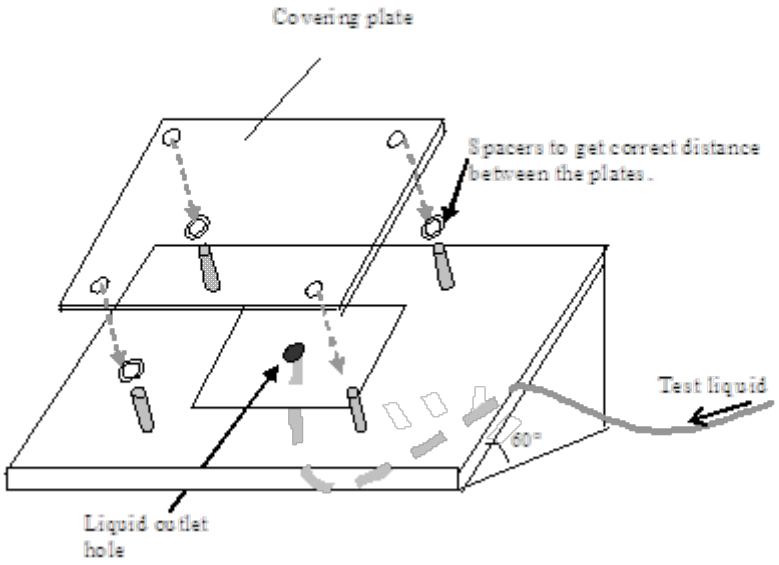

Figure 3.5: Sketch of inclined plane method

The resulting spreading pattern, as exemplified in Figure 3.6, was evaluated through visual examination.

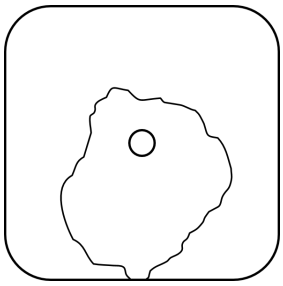

Figure 3.6: Example of a spreading pattern

3.3.5 Image analysis

To study the spreaing dynamics of test fluids in the airlaid material, a time-lapse sequence of images was obtained using an 8x speed smartphone camera. This approach allowed capturing the dynamic spreading process during the 4-hour test, resulting in a time-lapse video of approximately 30 minutes. The acquired images were then analysed using software such as Python and ImageJ.

Preprocessing techniques were applied to enhance image quality and facilitate subsequent analysis. These techniques included noise reduction, image sharpening, contrast adjustment, and image normalisation to improve clarity and consistency.

A region of interest (ROI) was defined in the acquired images to focus the analysis on the spreading pattern. The selection of the ROI was based on the location and extent of the liquid spread, ensuring it captured relevant information for further analysis.

Thresholding and contour detection techniques were then applied to separate the liquid spread area from the background and other regions in the images. This step enabled the isolation of the spreading pattern, facilitating precise measurement and characterisation.

Quantitative analysis was performed to identify the contour, area, and dimensions of the spreading pattern. A box with a fixed center position was fitted to the spreading area to quantify its length and width. The original center position remained as the box expanded with the spreading pattern, allowing for visualisation of the vertical spreading of the fluid in the material, as depicted in Figure 3.7.

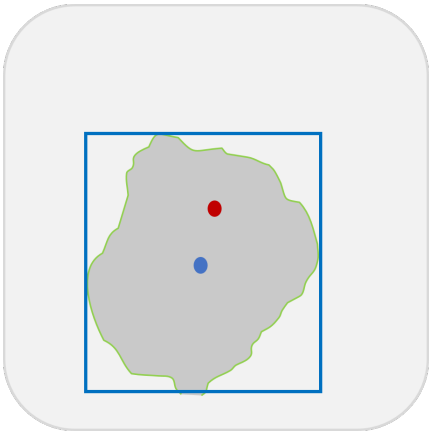

Figure 3.7: Quantitative analysis by fitting a box and center positions to the spreading pattern. The blue box follows the outline of the spreading pattern, the red dot is the original center position and the blue dot is the center position at the given time.

The analysed data were visually presented using graphs that effectively described and quantified the spreading behavior of the fluid within the airlaid material. Overall, this methodology provided a systematic approach to investigate and analyse the spreading patterns generated by liquid absorption into wound dressing materials using image analysis techniques.

4
Results and discussion

This section presents the findings of the experimental analyses conducted to assess the physico-chemical properties and spreading behavior of different test fluids. The objective of the study was to optimise SWF A to mimic the spreading behavior of SCS. Throughout the study, the composition of SWF A was modified by adjusting the protein content and adding surfactants to alter the content and nature of the surface-active components.

4.1 Physico-chemical properties

This section presents the results of the analysis done to assess various physico-chemical properties of the test fluids. Understanding these properties is crucial for evaluating the behavior and suitability of the test fluid in wound dressing applications. Each property provides unique insights into the characteristics and interactions of the test fluids, shedding light on their behavior within wound dressing materials.

4.1.1 pH

Figure 4.1 displays the results of the pH measurements. On average, the pH value was 6.38 for solution A, 7.45 for SCS, 7.42 for SWF A and SWF C, and 7.53 for SWF 20 and SWF B. SWF C was made by adding alkyl glucoside to SWF A, while SWF B was made by incorporating the same surfactant to SWF 20. The pH measurements indicate that the addition of surfactant does not significantly impact the pH of the fluids. The variations in pH observed among the protein solutions could potentially be attributed to inconsistencies in measuring the salt content during the preparation of the respective fluids. As mentioned in section (2.1.1), the pH in chronic wounds typically ranges between 7.15 and 8.9, which all protein solutions succeeded in doing, while solution A exhibited a pH more similar to that of healthy wounds. These observations highlight the influence of the test liquids formulation and composition on the pH.

Figure 4.1: pH values of the different wound fluid models

4.1.2 Conductivity

Figure 4.2 displays the results of the conductivity measurements, which showed variations among the fluids, indicating differences in ion content. Solution A had a significantly higher conductivity (15.42 mS/cm) compared to the protein solutions, suggesting that its ionic composition does not accurately mimic that of SCS. The conductivity of SWF 20 and SWF B (13.78 mS/cm respectively) was similar to that of SCS (13.89 mS/cm), indicating similar concentrations of free ions in the solutions. The conductivity of SWF A and SWF C (13.43 mS/cm respectively) was slightly lower than that of SCS, which could indicate that more salts are bound to the proteins in SWF A and SWF C compared to SCS. It could also be attributed to inconsistencies in measuring the salt content during the preparation of the respective fluids.

Figure 4.2: Conductivity values of the different would fluid models

4.1.3 Surface tension

Surface tension, which influences the spreading behavior of the fluids in wound dressings due to its direct correlation to capillary action, was evaluated. Figure 4.3 displays the average surface tension values obtained for the pre-existing test fluids and SWF A with altered BSA content (20 and 10 g/L BSA).

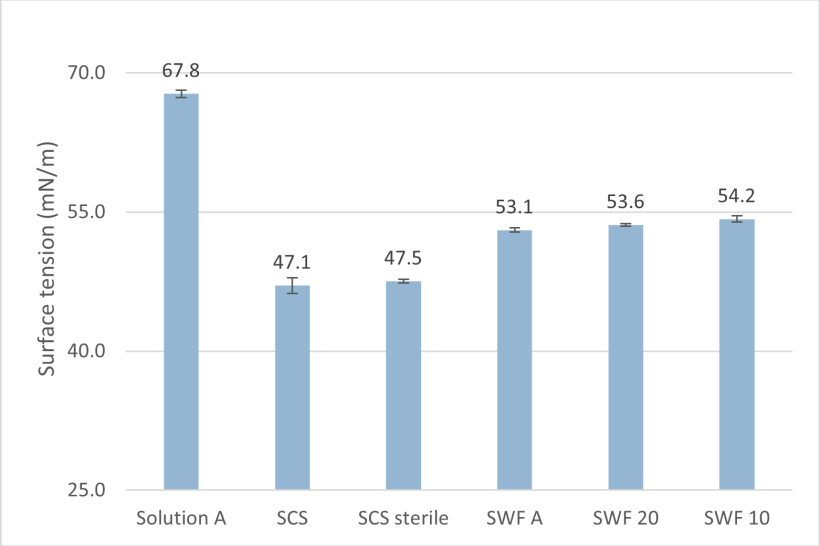

Figure 4.3: Average surface tension values of the different wound fluid models

Among the pre-existing fluids, it is evident that SCS exhibited the lowest surface tension value (47.1 mN/m). In comparison, SWF A demonstrated a somewhat higher surface tension value (53.1 mN/m), while solution A exhibited the highest value (67.8 mN/m). This difference in surface tension can be attributed to the absence of surface-active components in solution A, resulting in a higher surface tension similar to that of water (73mN/m). The higher surface tension of SWF A compared to SCS suggests that SWF A would exhibit a larger capillary action and thereby counteract gravity to a greater extent in a wound dressing material, as observed in previous studies mentioned in section (2.3). Additionally, it is worth noting that sterilised SCS showed a slightly higher surface tension (47.5 mN/m) compared to unfiltered SCS, indicating that the sterile filtration process may remove some surface active components. However, the difference in surface tension is negligible and is unlikely to have a significant impact on the spreading behavior, or could potentially be attributed to measurement errors.

The decreased BSA content of SWF 20 and SWF 10 induced a negligible increase of the average surface tension, 53.6 and 54.2 mN/m respectively, compared to SWF A. However, the decreasing BSA content did affect the dynamic surface tension, as demonstrated in Figure 4.4. The dynamic surface tension of SCS decreased approximately 1 mN/m before reaching an equilibrium, while the dynamic surface tension of SWF A decreased approximately 4 mN/m and did not reach an equilibrium during the measurement time. Although, as the BSA content decreased, the dynamic surface tension approached similar dynamics to SCS. This could be explained by

a faster surface adsorption rate of the proteins at low BSA concentrations, due to more rapid diffusion of the proteins to the interface compared to a solution with higher BSA concentration.

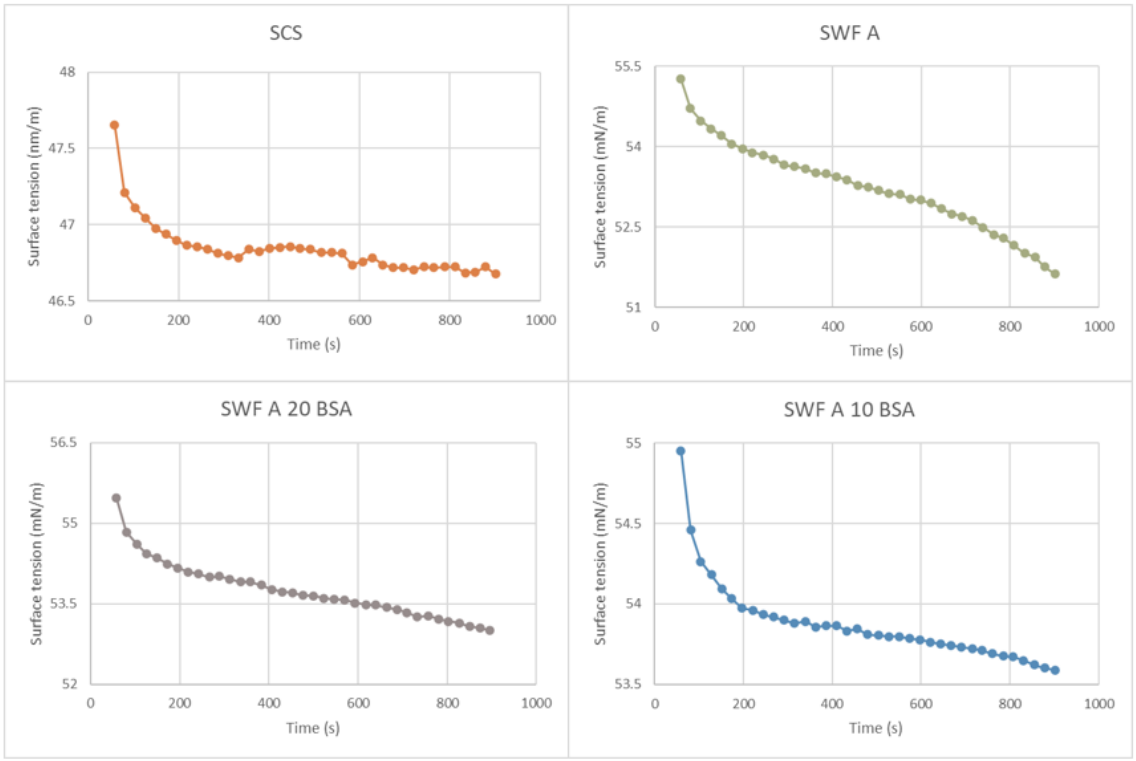

Figure 4.4: Dynamic surface tension of hte different wound fluid models

As mentioned in previous sections, real wound exudate contains a total protein content of 34 g/L, with BSA accounting for 20g/L of this total protein content. Therefore, both SWF A (with a total protein content similar to wound exudate) and SWF 20 (with a BSA content similar to wound exudate) were selected for further study and optimisation. A surfactant (alkyl glucoside) was added to the SWFs to mimic the inherent complexity of SCS with its broader range of serum proteins and natural presence of biosurfactants in the fluid. Furthermore, the addition of surfactant to the SWFs aids in emulating the surface tension of SCS. Figure 4.5 displays the range of investigated surfactant concentrations added to SWF 20. A surface tension similar to SCS (47.1 mN/m) was reached at an AG concentration of approximately 0.04%. Based on these findings, a new test fluid, SWF B, was formulated with a BSA content of 20 g/L and a 0.04% weight concentration of alkyl glucoside.

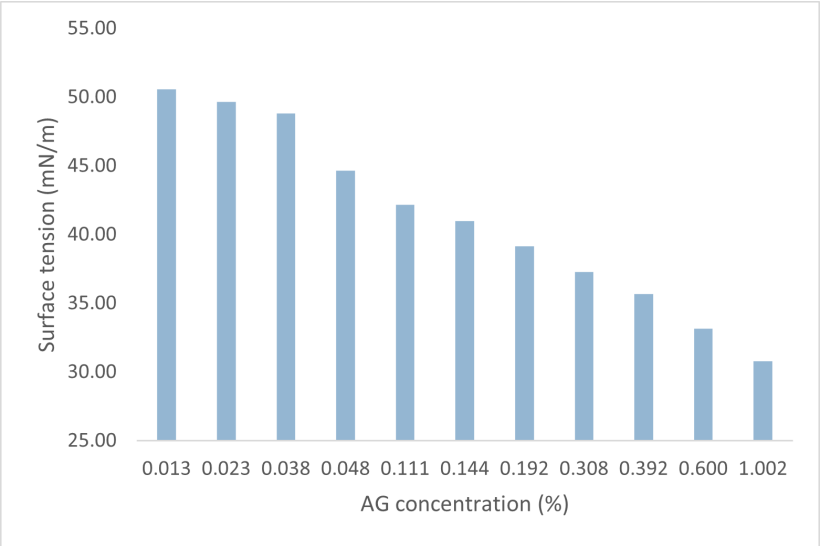

Figure 4.5: Surface tension of SWF 20 with varying AG concentration

The dynamic surface tension curve of SWF 20 with varying surfactant concentration approached that of SCS at a surfactant concentration of 0.05 % AG, as depicted in Figure 4.6. This indicates that the addition of surfactant affects the dynamics of the surface active components in the fluid and that the AG concentration needed to simulate the dynamic surface tension of SCS is close to the AG concentration required to reach an average surface tension similar to SCS. Surfactants are smaller molecules than proteins and can therefore diffuse to the interface more rapidly, thus causing the surface tension to reach a plateau faster compared to when only BSA is present.

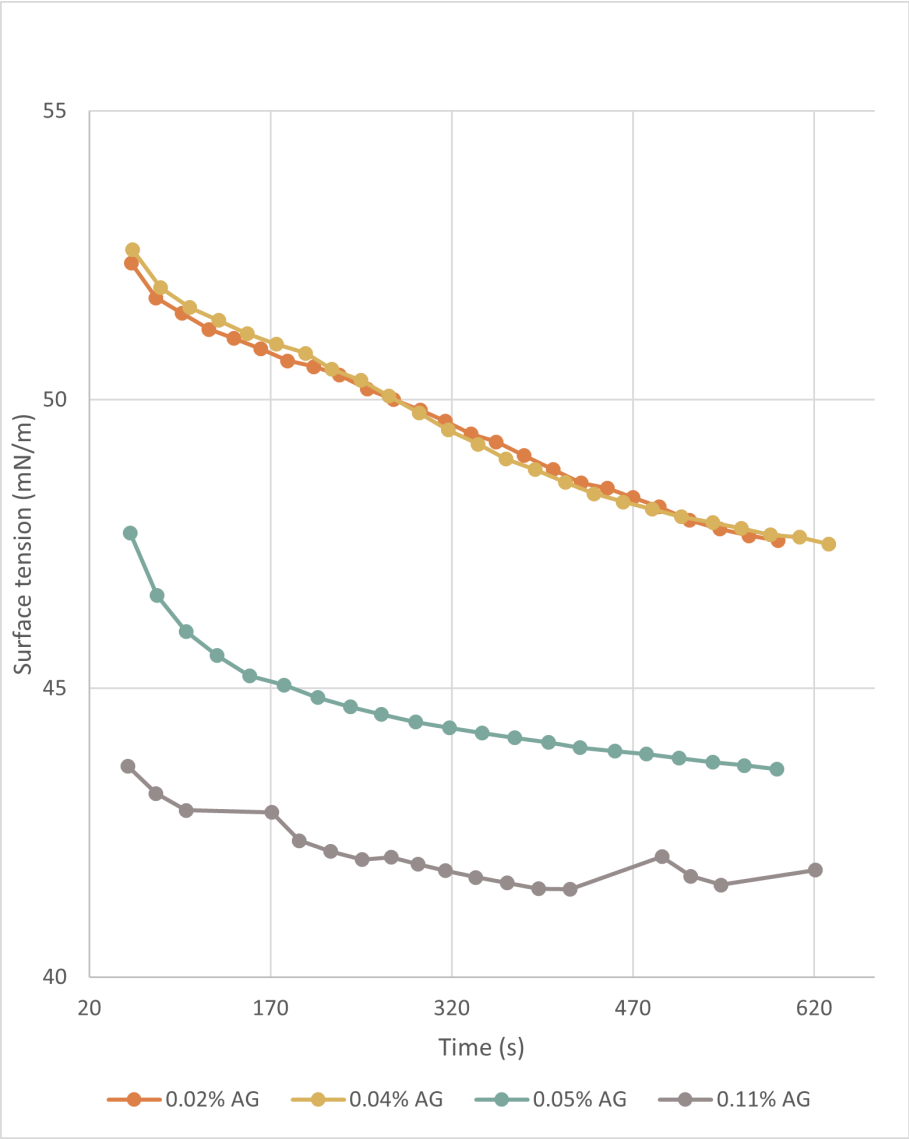

Figure 4.6: Dynamic surface tension of SWF 20 with varying surfactant concentration

The surface tension measurements SWF 20 with surfactant narrowed down the AG concentration range required in SWF A for establishing a surface tension similar to that of SCS. Figure 4.7 illustrates the range of investigated surfactant concentrations, where a surface tension similar to that of SCS (47.1 mN/m) was reached at approximately 0.05 % AG. Based on these findings, a new test fluid (SWF C) was formulated with the original BSA content of 34 g/L BSA and 0.05 weight % alkyl glucoside.

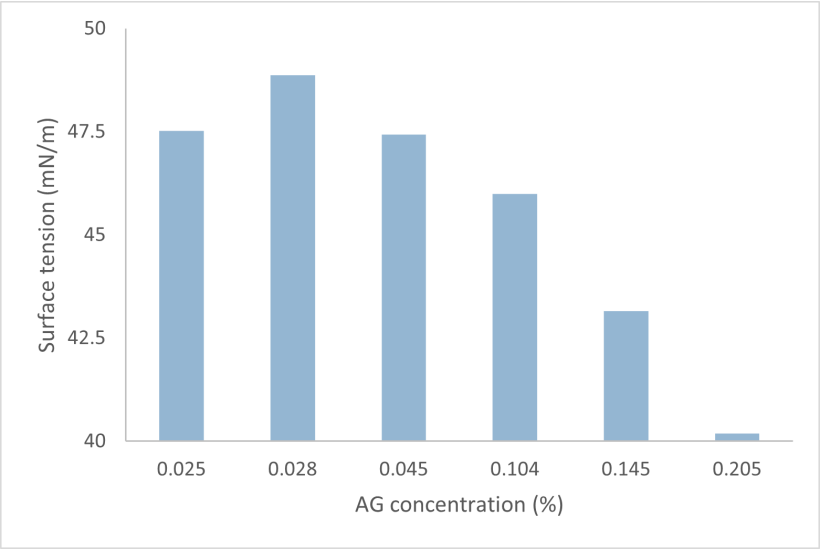

Figure 4.7: Surface tension of SWF A with varying AG concentration

The dynamic surface tension curve of SWF A with varying surfactant concentration approached that of SCS at a surfactant concentration of 0.145 % AG, as shown in Figure 4.6. As with SWF 20, the addition of surfactant to SWF A appears to affect the dynamics of the surface active components in the fluid. However, the AG concentration needed to simulate the dynamic surface tension of SCS is significantly higher than the AG concentration required to reach an average surface tension similar to SCS. This observation suggests that at higher BSA concentrations, such as in SWF A, the proteins may have a dominant role in interfacial adsorption, requiring a higher AG concentration for the surfactant to effectively occupy the interface. However, the interplay between proteins and surfactants in the fluid is complex and can not be conclusively analysed through surface tension studies alone.

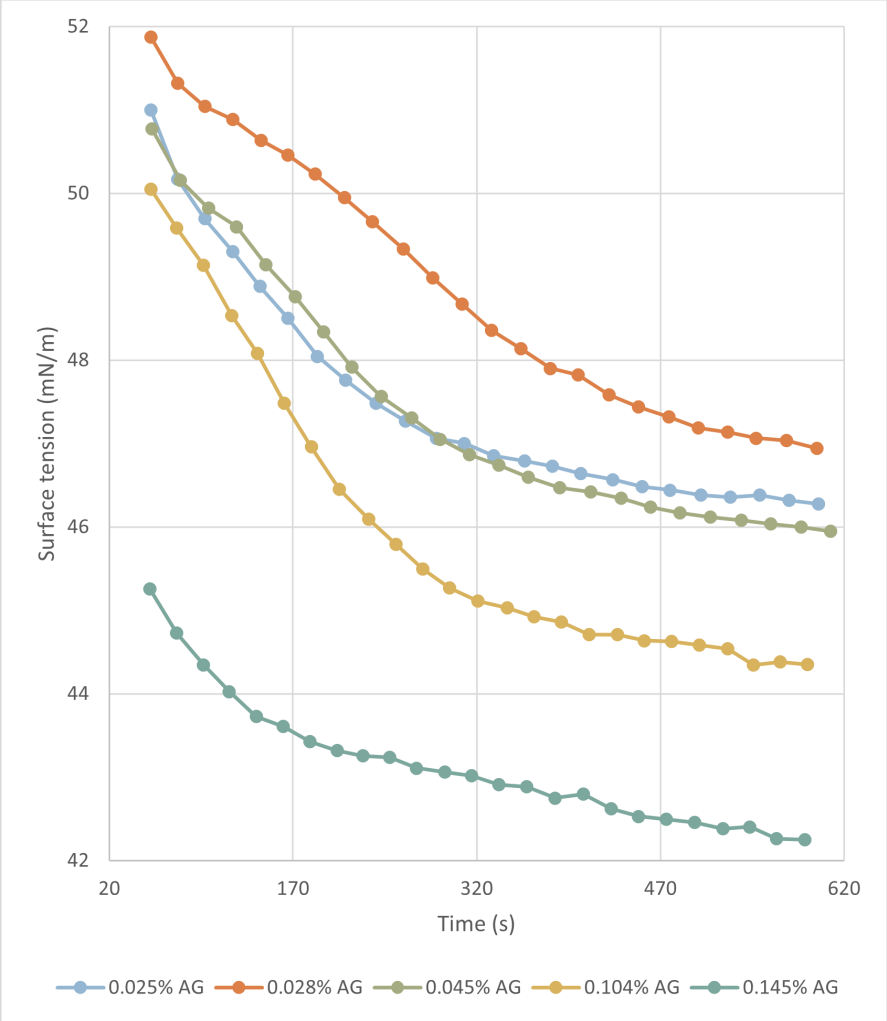

Figure 4.8: Dynamic surface tension of SWF A with varying surfactant concentration

4.1.4 Viscosity

Viscosity is a crucial parameter that influences the flow and spreading behavior of the fluid. Figure 4.9 displays the viscosity values obtained for the pre-existing test fluids, as well as SWF A with altered BSA content (20 and 10 g/L BSA). The results showed that all protein solutions have a somewhat similar viscosity (1.5-1.6 cps), thus it was concluded that viscosity of these fluids is unlikely to have a large impact on their differences in spreading behavior. However, it is important to note that this experiment was performed at room temperature. Therefore, the findings do not provide specific insights into the influence of temperature on viscosity, which could be significant in real-life scenarios. Further studies involving temperature-controlled experiments and measurements with an increasing shear would be necessary to investigate the relationship between temperature, shear, and viscosity in these test fluids.

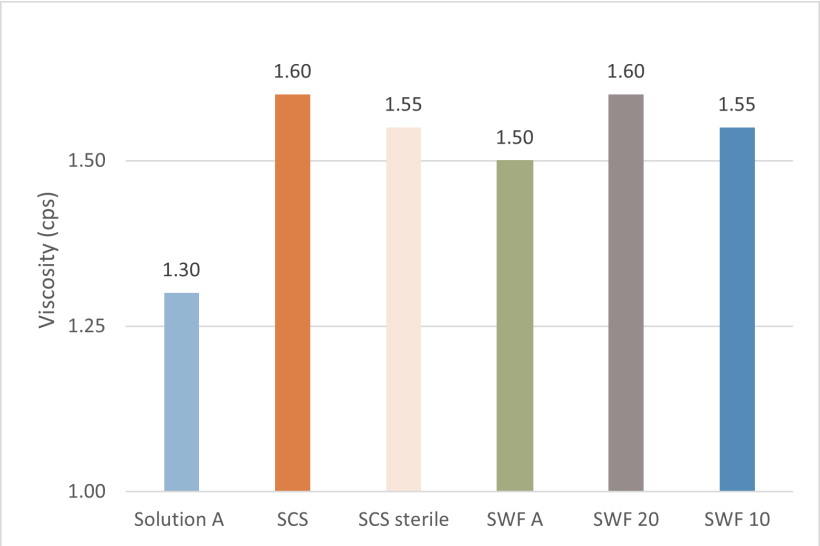

Figure 4.9: Viscosity of the model would fluids

4.1.5 Contact angle

Contact angle allows to characterises the wetting behavior of a liquid on a solid surface, providing insights into the interaction between the test fluids and the solid substrate. Figure 4.10 displays the contact angle values obtained for the test fluids on the hydrophobic Safetac silicone substrate. A low contact angle would indicate good wetting of the substrate, while a high contact angle would indicate poor wetting. However, it is important to note that poor wetting of the hydrophobic silicone correlates to good wetting of the hydrophilic airlaid material, which is the actual material of interest with regards to spreading behavior.

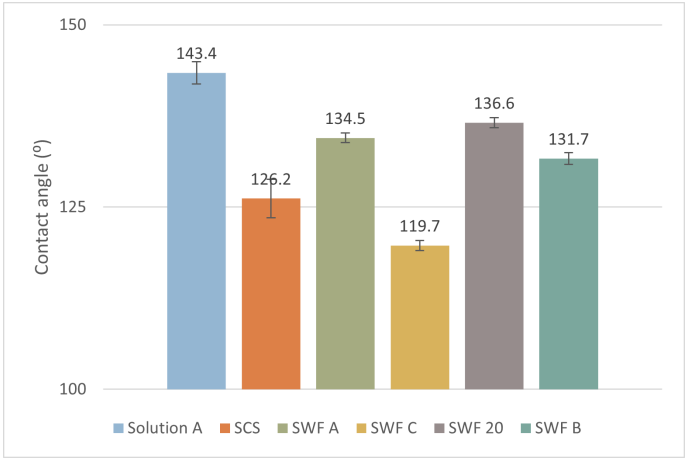

Figure 4.10: Contact angle of the model wound fluids

From the results, it can be observed that among the test fluids without surfactant, solution A had the highest contact angle (143.4), followed by SWF 20 (136.6), then SWF A (134.5), and lastly SCS (126.2). A lower contact angle correlates with that the fluid has a lower surface tension, which may be a result of the concentration and

nature of the proteins. Human serum albumin is known to be more surface active than bovine serum albumin, it stands to reason that the same would be true for the horse serum albumin in SCS.

The surfactant solutions, SWF B and SWF C, have the same surface tension as SCS, yet they do not display the same contact angle. The contact angle of SWF C (119.7) is significantly lower than that of SWF B (131.7), which could be a result of differing BSA content and protein-surfactant interactions. Considering that the surface tension of both fluids should be approximately the same, and the interfacial tension between the solid substrate and air should be constant, it is likely that the BSA content and protein-surfactant interactions impact the interfacial tension between the fluid and the substrate according to Young's equation (Eq. 2.1).

The observed differences in contact angle values indicate the potential for further optimisation of the test fluid compositions to better mimic the wetting and spreading behavior of SCS. Further investigation into the correlation between contact angle and spreading behavior in the airlaid material, as well as the influence of other physicochemical properties, will be critical for understanding the interactions between the test fluids and the wound dressing material.

4.1.6 Protein composition

SDS-PAGE analysis was performed to evaluate the protein composition and molecular weight distribution in the test fluids. The protein composition was assessed by analysing the band intensities and migration patterns, while the molecular weights were estimated based on their migration positions relative to protein standards.

Figure 4.11 displays the SDS-PAGE gel image of SCS, SWF A, SWF B, and SWF C. The image reveals distinct protein bands in all test fluids, indicating the presence of proteins in the samples. The most prominent band, observed at approximately 66 kDa, corresponds to the serum albumin proteins. This confirms that the major protein component in all test fluids is serum albumin.

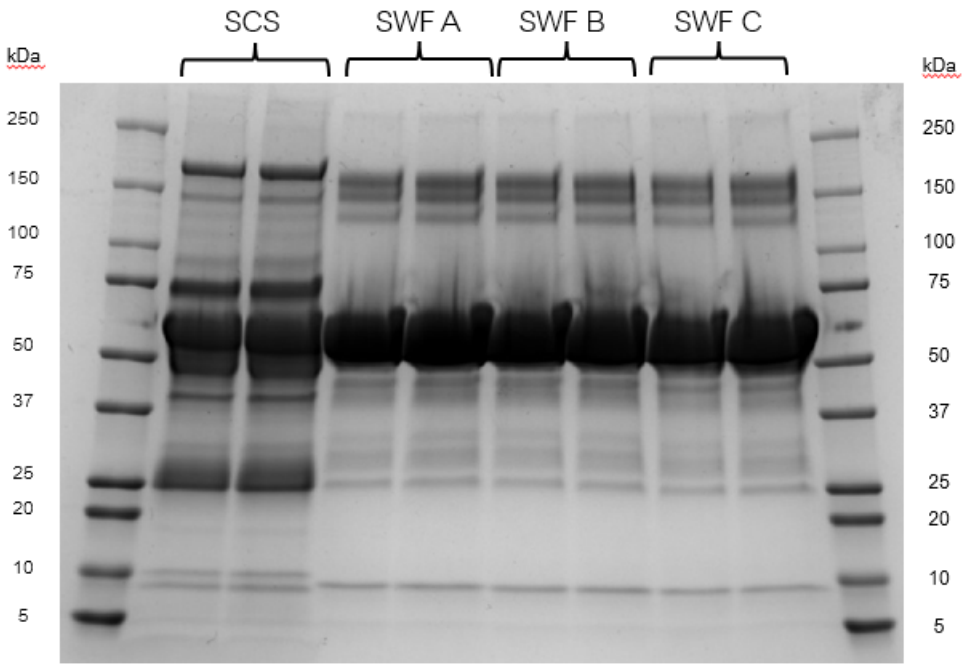

Figure 4.11: SDS-PAGE analysis results of the wound fluids

Overall, the protein composition and molecular weight distribution of all SWFs appear to be similar, as evidenced by their comparable migration patterns and band intensities. These results are expected since the SWFs share similar compositions with variations in BSA content and the addition of surfactant. The lack of significant differences in protein composition and molecular weight distribution between the SWFs indicates that altering the BSA content and incorporating surfactants did not significantly impact these aspects of the test fluids.

In contrast, SCS exhibited a different migration pattern and band intensities compared to the SWFs. This disparity can be attributed to the fact that SCS contains a broader range of serum proteins compared to the SWFs. For instance, SCS displayed bands at approximately 75 and 10 kDa that were not observed in the SWFs. Understanding the influence of these specific molecular weights on the physico-chemical properties and spreading behavior of the fluids would require further investigation.

4.2 Spreading behavior

This section presents the findings from the experiments conducted to evaluate the spreading behavior of the test fluids within wound dressing materials, with a primary focus on airlaid. Understanding the spreading behavior is crucial for assessing the performance and effectiveness of the test fluids in mimicking real wound exudate. The spreading behavior was evaluated using a combination of techniques, including wicking tests, the FLUHTE simulated wound model, the inclined plane method, and time-lapse image analysis for quantification of spreading patterns. These approaches provided comprehensive insights into the dynamics and distribution patterns of the

test fluids within the wound dressing materials. SEM was used to look at the potential modification of the wound dressings after exposure to the model fluids.

4.2.1 Wicking

Wicking tests were conducted to gain insights into the capillary action and fluid transport properties of the wound dressings. The test measured the distance traveled by the test fluids within different materials over a 5-minute time period, as well as the absorbed fluid weights. The results revealed variations in the wicking behavior among the different fluids and materials tested.

As mentioned in section 3.3.1, water and ethanol were used to assess the wicking behavior of different materials (PU foam, airlaid, filter paper, and printer paper). Figure 4.12 displays the capillary action and absorbed fluid weight of each respective fluid in the different materials. Notably, the airlaid and filter paper materials exhibited distinct differences in both capillary action and absorbed fluid weight between the liquids, while PU foam and printer paper did not. Hence, airlaid and filter paper were identified as suitable materials for demonstrating differences in wicking behavior between fluids with different surface tensions. Interestingly, the difference in absorbed fluid weight seemed to correspond to the difference in surface tension between the fluids, whereas the difference in capillary action did not exhibit the same correlation for the airlaid. This inconsistency could be attributed to factors such as pore size distribution and variations in material composition.

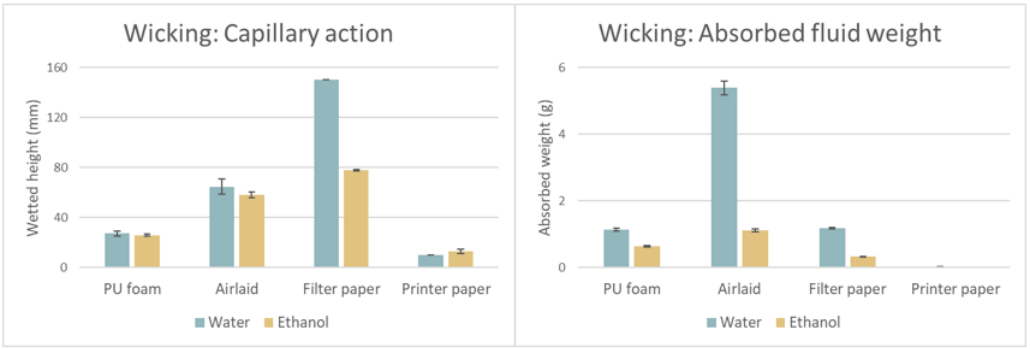

Figure 4.12: Wicking test of water and ethanol to assess the wicking behavior of PU foam, airlaid, filter paper, and printer paper

Figure 4.13 displays the capillary action and absorbed fluid weight of the pre-existing test fluids (solution A, SCS, and SWF A), as well as SWF A with altered BSA content (20 and 10 g/L BSA). Among the pre-existing test fluids, solution A demonstrated the greatest wicking, SCS exhibited the lowest wicking, and SWF A exhibited an intermediate wicking properties compared to SCS, in terms of both capillary action and absorbed fluid weight. This correlates to the measured surface tension of the fluids observed in section 4.1.3. The greater wicking properties of SWF A compared to SCS indicate its ability to counteract gravity to a greater extent, as observed in previous studies (see section (2.3)). The results also showed that wicking increased when the amount of surface active components decreased, as expected.

For instance, solution A, lacking surface active components, exhibited the greatest wicking, and SWF 10 displayed a greater wicking than SWF 20, which in turn had a greater wicking than SWF A.

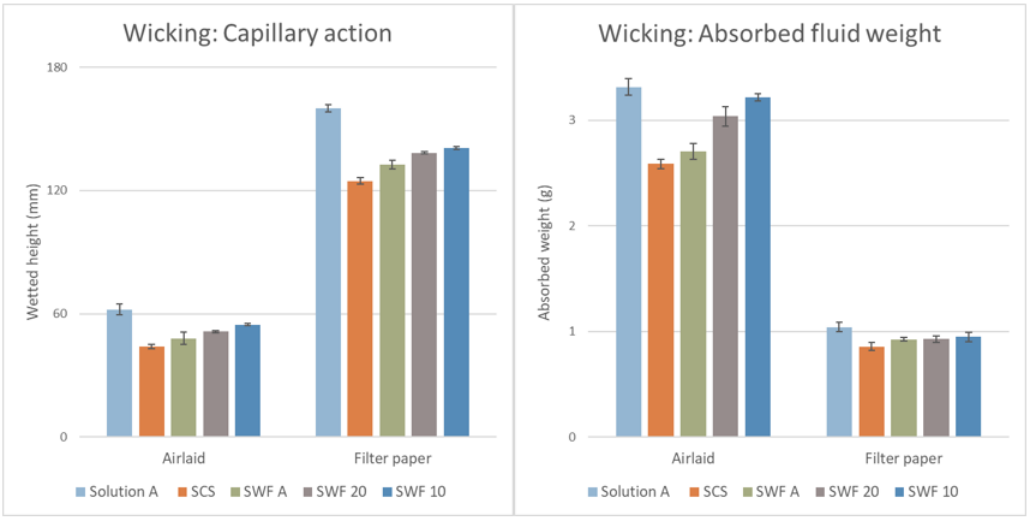

Figure 4.13: Wicking test of solution A, SCS, SWF A, SWF 20 and SWF 10, in airlaid and filter paper material

Figure 4.14 displays the capillary action and absorbed fluid weight of SCS, SWF A, SWF C, and SWF B. Although the surface tensions of SWF C and SWF B were approximately the same as that of SCS due to the addition of surfactant, their wicking behavior was more similar to SWF A in terms of capillary action in both materials. The same was observed with regards to the absorbed fluid weight in the airlaid material, however, the filter paper demonstrated an absorbed fluid weight of SWF C and SWF B that was more similar to SCS. These findings indicate that other factors than surface tension affect the wicking of fluids. For instance, there could be material variations between different replicates, and the differences in protein composition between SCS and the SWFs might induce different fluid-material interactions, as a result of e.g. adsorption.

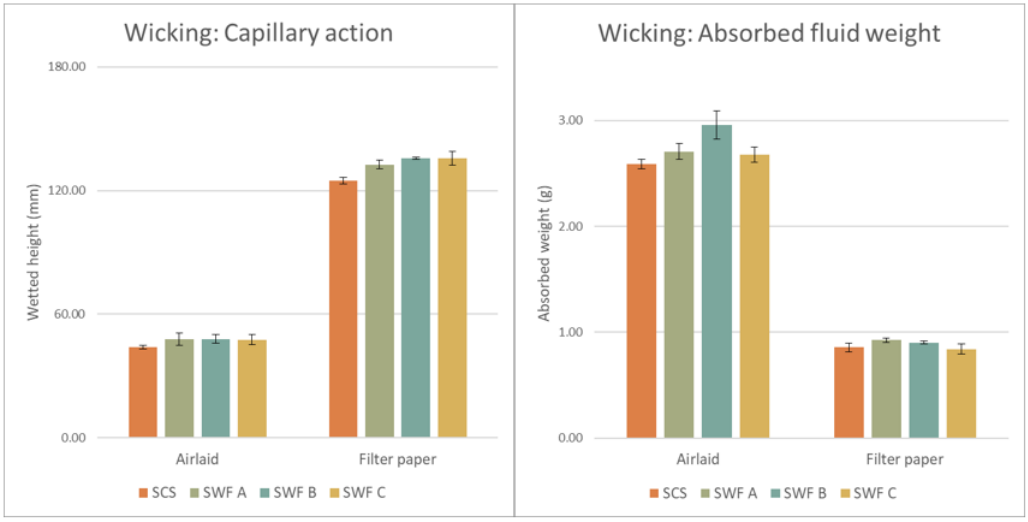

Figure 4.14: Wicking test of SCS, SWF A, SWF C and B, in airlaid and filter paper material

4.2.2 FLUHTE

FLUHTE is a clinically relevant simulated wound model for chronic leg ulcers that was employed to study the spreading behavior of the test fluids in the airlaid material. The method encompasses both mass- and heat transfer processes that are similar to those found in real chronic wounds.

As mentioned in section 2.3, gravitational effects typically leads to a spreading pattern which forces the wound exudate towards the bottom border of the dressing. The spreading behavior of SCS is very similar to that of real chronic wound exudate, whereas SWF A has been observed to counteract gravity to a greater extent by spreading more uniformly around the wound area.

The spreading behavior of SWF B was examined in FLUHTE, as shown in Figure 4.15. Three replicates were performed, where the first two were placed in the machine direction (consistent with previous studies), while the third replicate was placed in the cross-direction. Both replicates placed in the machine direction display a spreading behavior similar to that of SCS, as the fluid has been forced towards the bottom border of the dressing material. This indicates that SWF B succeeds in mimicking SCS in terms of spreading patterns, which suggests that BSA content and surface tension are crucial properties for the spreading behavior of test fluids. However, the replicate placed cross-directionally did not display the same spreading behavior as the fluid spread more uniformly around the outlet holes of the FLUHTE and had not been forced toward the bottom border of the material. These findings indicate that the fiber direction of the material affects the spreading pattern of the test fluid, hence the placement of the wound dressing could impact its effectiveness in wound management.

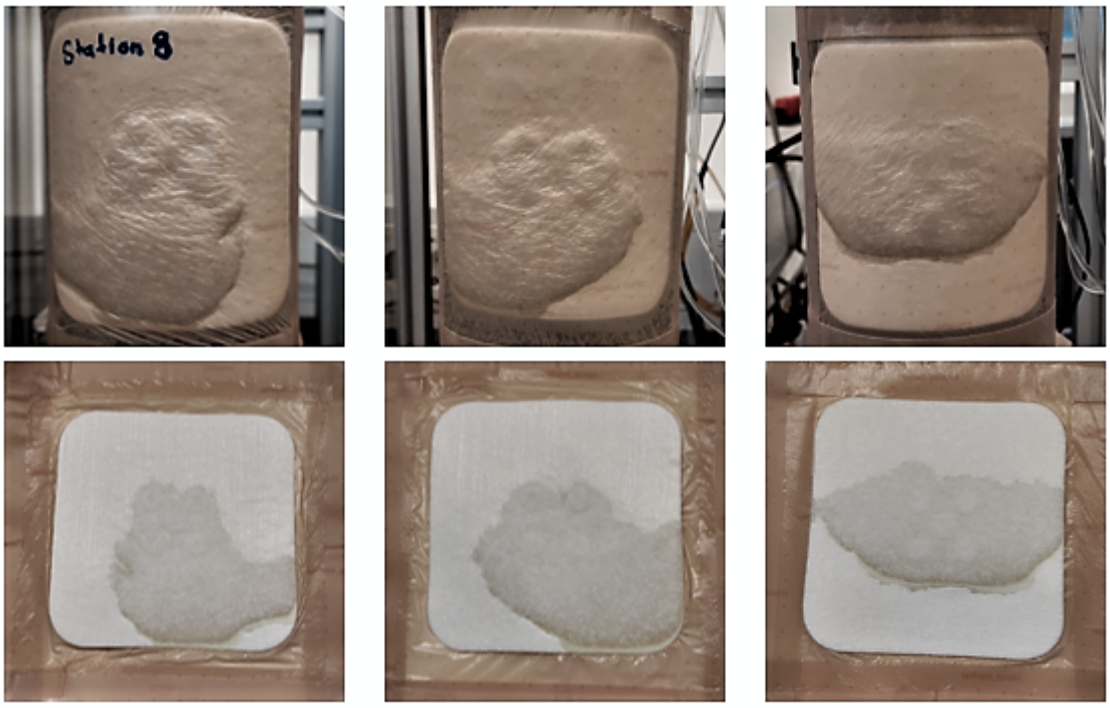

Figure 4.15: Spreading behavior of SWF B in FLUHTE, where the top row shows the back of the dressing and the bottom row shows the front of it.

To investigate the effect of surface tension and surfactant concentration on the spreading behavior in airlaid material, SWF with 20 g/L BSA and 1% alkyl glucoside was used in FLUHTE. As stated in section 4.1.3, the surface tension of such a fluid was shown to be 30.8 mN/m, contrasting the surface tension of SCS (47.1 mN/m). Since surface tension is directly correlated to capillary action, this fluid should display lower capillary action than both SCS, SWF A, and SWF B, which is precisely what Figure 4.16 shows. Both replicates show that the fluid did not spread horizontally from the outlet holes of the FLUHTE, instead most of the fluid had been forced to the bottom border of the dressing material. The bottom border seems to act as a barrier for the fluid and forced it to spread horizontally. These findings highlight the importance of having a test fluid with a surface tension similar to that of SCS and real wound exudate.

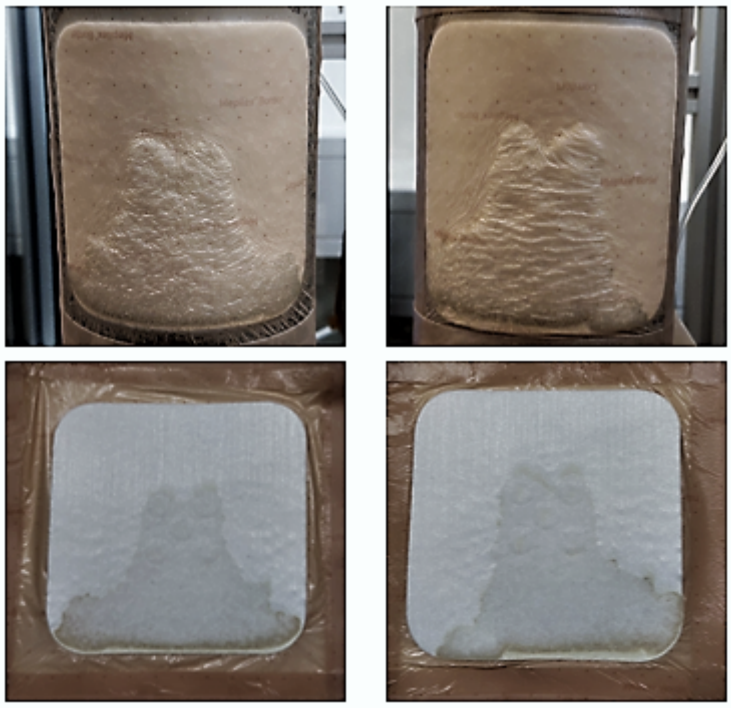

Figure 4.16: Spreading behavior of SWF 20 g/L BSA + 1.0% AG in FLUHTE, where the top row shows the back of the dressing and the bottom row shows the front of it.

The spreading behavior of SWF C was also examined in FLUHTE, as shown in Figure 4.17. SWF C was formulated to have the same composition as SWF A, except for the addition of alkyl glucoside to achieve a surface tension similar to that of SCS. Figure 4.17 shows that SWF C counteracted gravitational effects more than SCS and SWF B.In two of three replicates, the fluid was not forced to the bottom border of the dressing material. Instead, BSA seems to aggregate and form a barrier that hinders the fluid from flowing downwards. This indicates that surface tension is not the only property affecting the spreading behavior, but the protein concentration, composition and stability appear to be of importance as well.

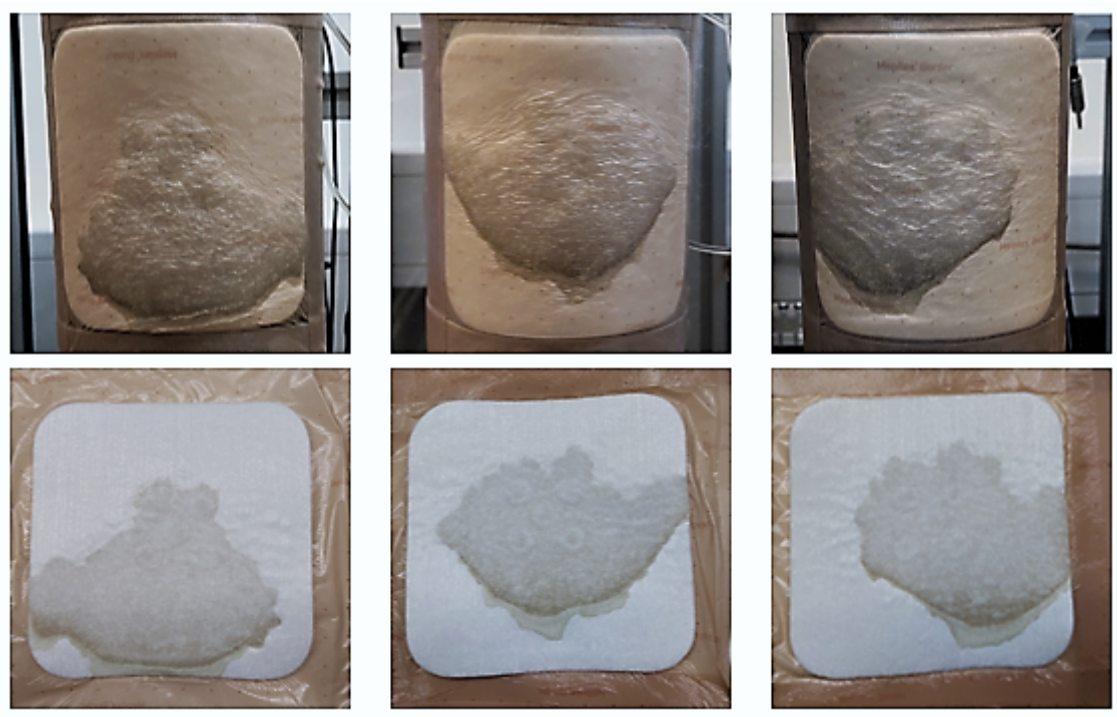

Figure 4.17: Spreading behavior of SWF C in FLUHTE, where the top row shows the back of the dressing and the bottom row shows the front of it.

According the results obtained from the FLUHTE experiments, the fluid content and the moisture vapour loss of the test fluids were calculated and analysed. The left chart in Figure 4.18 shows that SWF B and SWF C had a similar fluid content to SCS after a 24-hour run in FLUHTE, indicating how much liquid the material held. On the other hand, SWF 20 with 1% AG held noticeably less fluid. The right image displays that SWF B and SWF C had similar moisture vapour loss to SCS, meaning how much fluid had evaporated from the material. However, SWF 20 with 1% AG showed a higher evaporation. These findings suggest that a higher surfactant concentration leads to increased moisture vapour loss and reduced fluid content of the material. It is possible that the higher surfactant concentration causes the fluid to be forced towards the bottom border of the material to a greater extent than the other fluids. This higher contact area with the border of the dressing could result in a higher moisture vapour loss and reduced fluid retention.

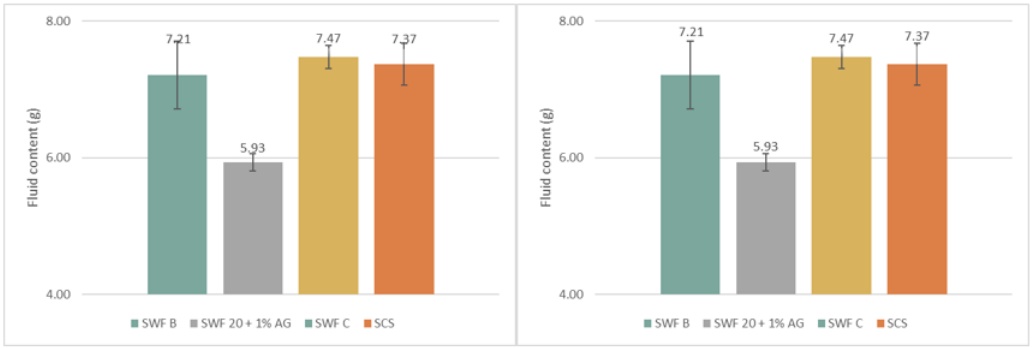

Figure 4.18: Fluid content and moisture vapour loss of test fluids after FLUHTE

It is worth noting that SWF B exhibited similar spreading behavior to SCS in the airlaid material during FLUHTE experiments. However, SWF B lacks 14 g/L of protein that is present in SCS. This raises the question of whether these proteins play a crucial role in other aspects of the dressing's behavior. While SWF B replicates the spreading behavior of SCS, further investigation is required to understand if there are any other differences in behavior between SWF B and SCS in other regards. Therefore, additional research is needed to explore the impact of protein content and other factors on the behavior of dressing materials and their overall effectiveness in wound fluid management.

4.2.3 SEM

One sample from the FLUHTE experiments of SWF C was collected and dried for examination using SEM with the purpose of visualising the hypothesized dried protein barrier that prevented fluid from flowing down in the material. Figure 4.19 presents several SEM images that provide insights into the composition and distribution of proteins within the material. Image 1 in Figure 4.19 shows the bottom crust of the barrier, which appears to be composed of aggregated protein flakes. Moving to image 2, a close-up view reveals that the protein flakes saturate the entire material, not just the surface. This suggests that the protein barrier extends throughout the material rather than being limited to the surface layer. Image 3-6 progress upwards in the material from the protein barrier. These images demonstrate a gradual decrease in abundance of protein flakes and eventually their complete disappearance as the location approaches the outlet holes of the FLUHTE. It is important to note that the absence of visible protein flakes does not necessarily imply the absence of protein aggregates, rather, it could indicate that they are either too small to be visualised at the magnification used or not visible at all. Another possibility is that the size of the protein and protein aggregates causes them to be forced downwards within the material due to gravitational effects.

Overall, the observations from SEM suggest that heat and mass transfer processes play a role in the evaporation of liquid and the formation of protein aggregates. As the liquid evaporates from the material, the protein and salt concentrations within the material increase and induce protein aggregation. These processes likely contribute to the creation of the protein barrier and its consequences on the fluid flow within the material. Further analysis and characterization of the protein aggregates, as well as a comprehensive understanding of the heat and mass transfer mechanisms, would provide valuable insights into the behavior and performance of the dressing material.

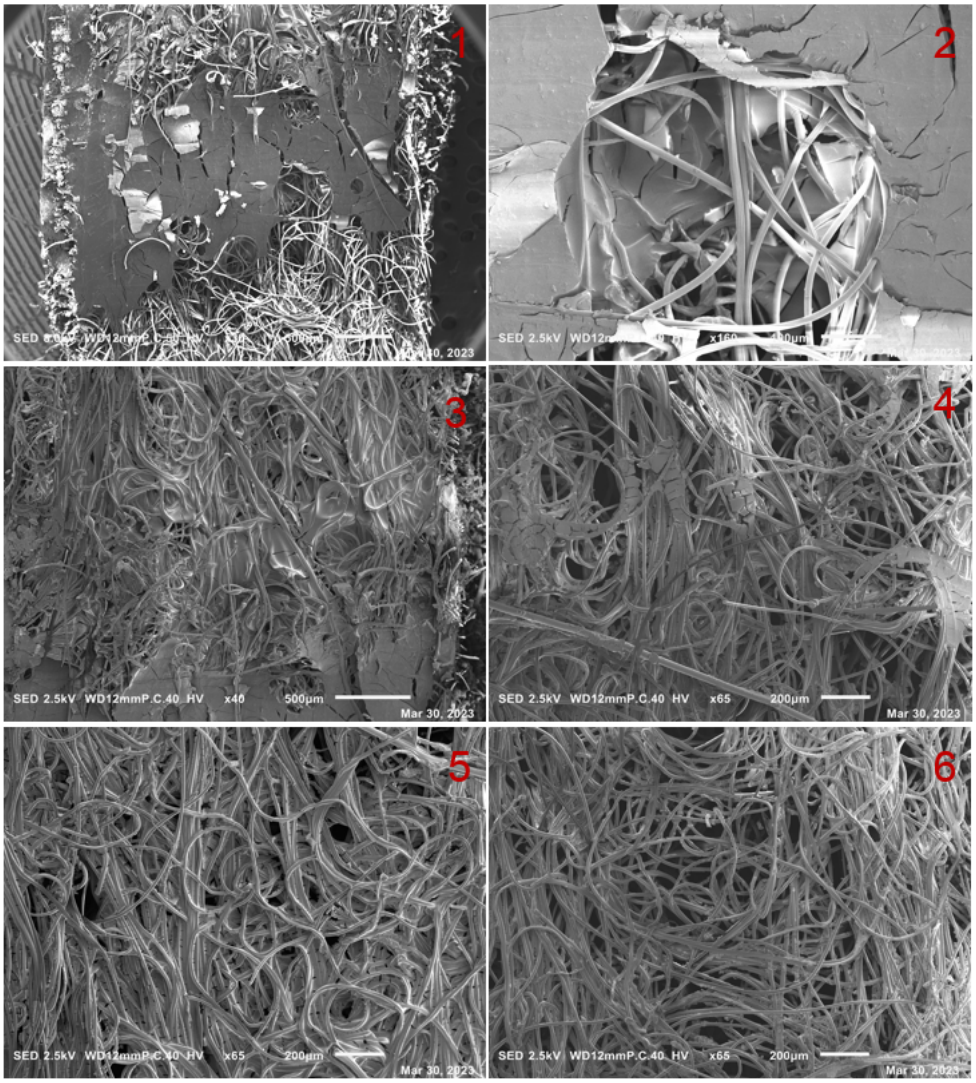

Figure 4.19: SEM images. 1: overview of the bottom crust of the dried protein barrier, 2: close-up view that shows the saturation of protein flakes throughout the material, 3-6: upward progression from the protein barrier that show a gradual decrease in abundance of protein flakes.

4.2.4 Inclined plane method

The inclined plane method was employed to study the spreading behavior of test fluids in wound dressing materials. Figure 4.20 shows the spreading behavior of SWF A, SWF C and SCS in Mepilex border flex attached to the inclined plane without the plexiglass plates to apply pressure. However, due to the presence of the backing film of the product, visual observations of the spreading patterns are limited, and there appears to be little to no difference between the fluids. This could be due to uneven adherence of the product to the plane, which could cause the fluid to flow downwards before even getting into contact with the dressing material. Alternatively, it could also be due to the lack of compression, which affects the structure of the material itself. To optimise the methodology, subsequent experiments focused

solely on the airlaid material, and plexiglass plates were attached to apply a pressure of 40 mmHg, equivalent to the pressure used in FLUHTE experiments.

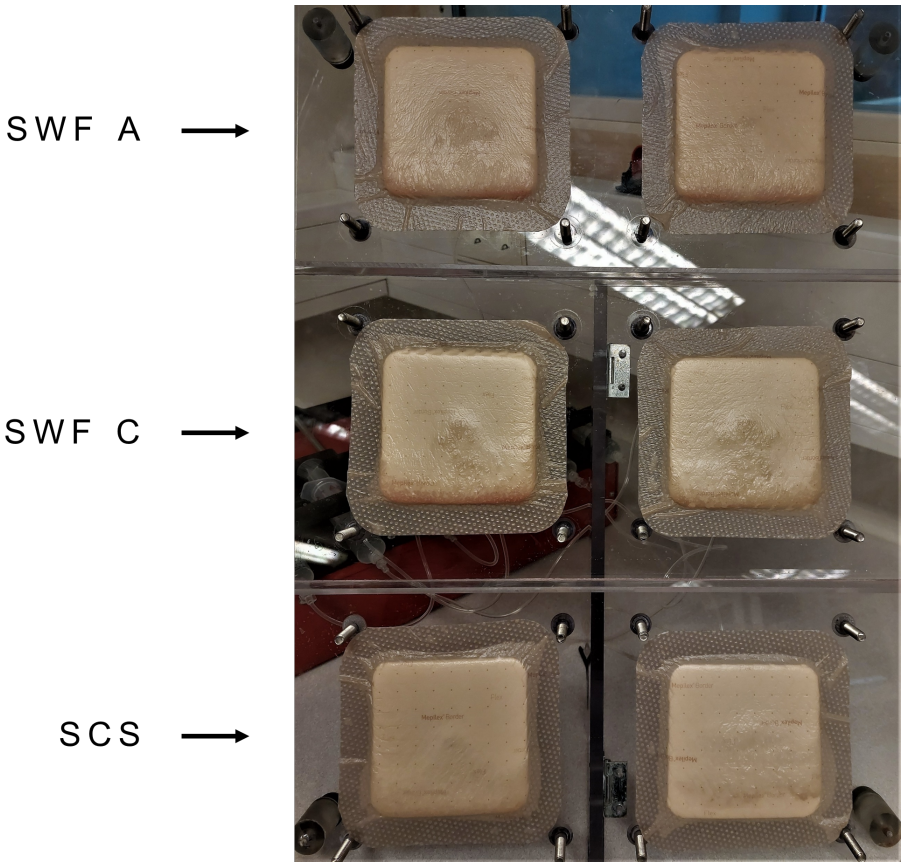

Figure 4.20: Spreading behavior of SWF A, SWF C, and SCS in Mepilex border flex

Figure 4.21 displays the spreading behavior of SWF A, SCS, SWF C, and SWF B in airlaid material using the inclined plane method. By focusing on the airlaid material and applying pressure, it became significantly easier to visualise the spreading patterns. The application of pressure seems to play a vital role in inducing different spreading behaviors of the fluids. This is most likely due to structural changes of the material due to compression.

Some general trends could be observed visually. SWF A exhibited a more uniform spreading pattern around the outlet hole compared to the other fluids, which tended to spread more vertically and were forced towards the bottom border of the material. Currently, the difference in spreading patterns between the SWF B and SWF C could be attributed to either material variations or actual distinctions between the fluids. Conducting more replicates would help minimise the impact of material variations and establish which fluid is more similar to SCS in terms of spreading patterns. Furthermore, relying solely on visual observations made it challenging to analyse the spreading patterns accurately. Quantification of spreading patterns through image analysis was therefore used to obtain more quantitative results.

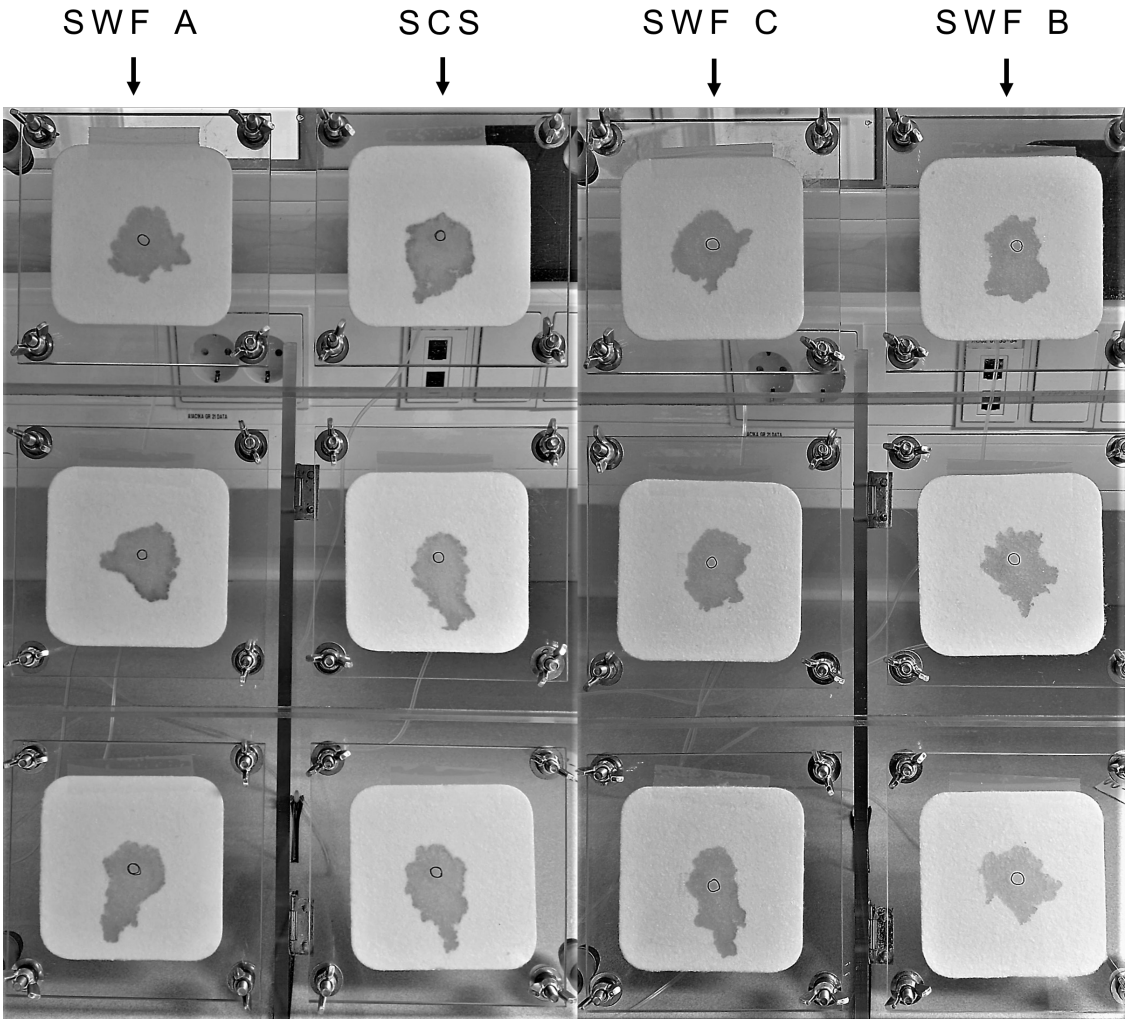

Figure 4.21: Spreading behavior of SWF A, SCS, SWF C, and SWF B in inclined plane, where row 1-3 are the three different replications per fluid.

Unlike the FLUTE experiments, which included both mass- and heat transfer processes, the inclined plane method encompasses only mass transfer processes since the experiments were conducted at room temperature and the plexiglass plates prevented fluid evaporation. Consequently, there were no visible formation of protein barriers or protein aggregation, as observed in the FLUHTE experiments.

4.2.5 Spreading dynamics and pattern quantification

The dynamic spreading process of the test fluids was analysed using the inclined plane method, and image analysis was employed to quantify the spreading process over time. This section presents the results obtained from the image analysis, including the measurement of various parameters and the characterisation of the spreading behavior.

To capture the dynamic spreading process, a time-lapse series of images was recorded.

These images were then subjected to image analysis techniques to extract relevant information and to quantify the spreading behavior. As explained in the methodology section about image analysis (section 3.3.5), a box was fitted to the spreading pattern to acquire its dynamic length and width. The original and dynamic center position of the box was also displayed to visualise how the spreading pattern deviated from uniformity. If the fluid spread uniformly from the outlet hole, the center position would remain the same throughout the dynamic process, but if the fluid did not spread uniformly the center position would deviate from its original position.

Figure 4.22 displays four images per fluid from the time-lapse that illustrates the dynamic spreading processes of SWF A, SCS, SWF C, and SWF B in the airlaid material. Visual observation shows that SWF A had the most uniform spreading pattern throughout the process, while SCS, SWF C, and SWF B had a more vertical spreading pattern.

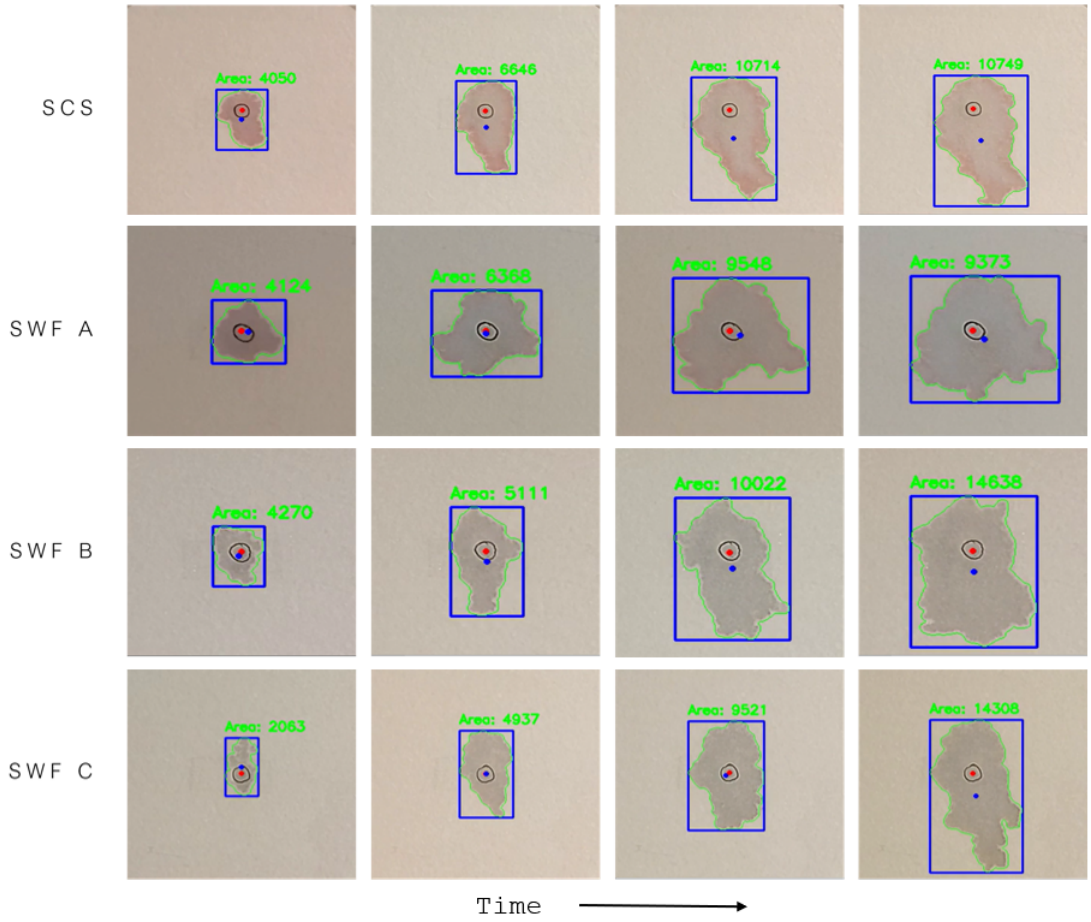

Figure 4.22: Dynamic spreading process of SCS, SWF A, SWF B, and SWF C, in airlaid material via the inclined plane method. The blue boxes are fitted to the spreading pattern, the red dots denotes the original center position, and the blue dots is the current center position.

Figure 4.23 indicates that the center position of SWF A was more constant than the other fluids. The center position of SCS and SWF C decreased significantly more

and followed similar trends. The trend for the center position of SWF B was somewhat in between that of SCS and SWF A. This quantitative analysis of the dynamic spreading patterns confirms that SWF A has a more uniform spreading than the other fluids, which have a more vertical spreading (to different degrees). It is important to note that this analysis was performed on one of the replicates, the trends might look different for other replicates. Furthermore, this type of quantification only considers the vertical change (y-axis) of the center position, not the horizontal. Visual observations show that the horizontal spreading also differs between fluids, which be of interest to quantify in further studies.

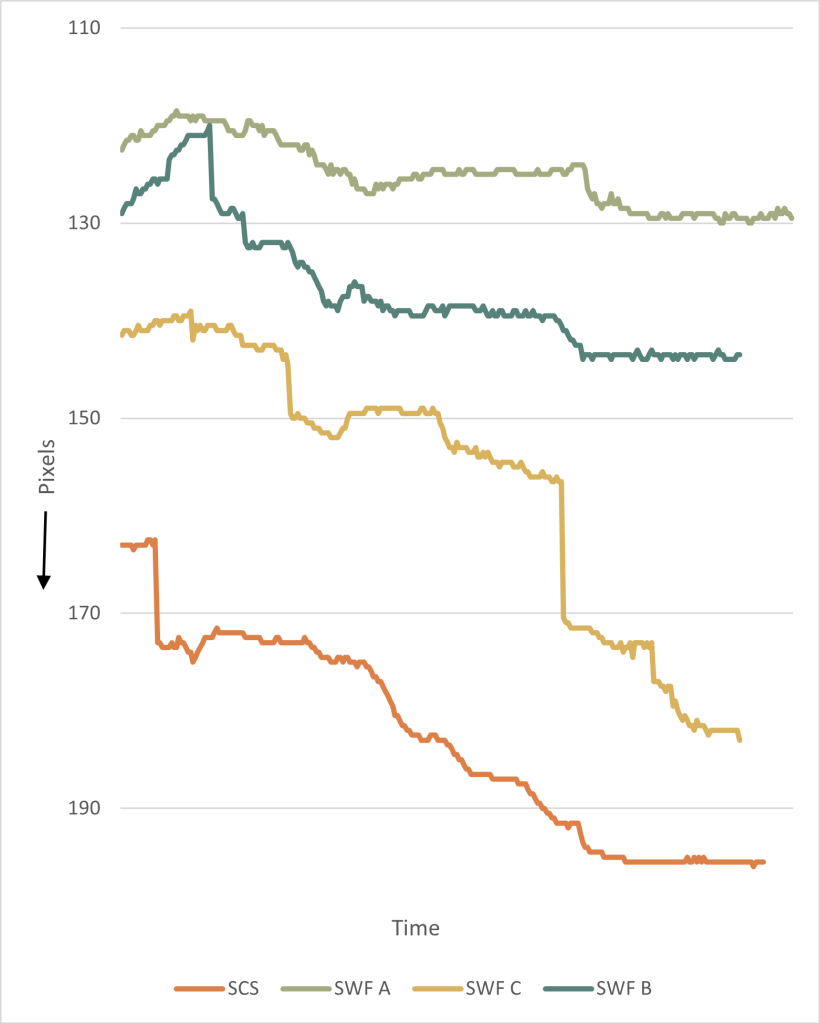

Figure 4.23: Center position as a function of time

Another method for pattern quantification involves the aspect ratio of the fitted boxes. A uniform spreading pattern would result in an aspect ratio equal to 1, however, if the fluid spreads more in the vertical direction than the horizontal, the aspect ratio is < 1. Oppositely, if the fluid spreads more in the horizontal direction than the vertical, the aspect ratio is > 1. Figure 4.24 displays that the aspect ratio of SWF A is > 1, while the aspect ratios of SCS, SWF C, and SWF B are < 1. The aspect ratios vary over the dynamic process, but as Figure 4.24 shows, the dynamic aspect ratios of SCS, SWF C, and SWF B are somewhat similar and intersect sev-

eral times. However, the end point shows that the aspect ratio is lowest for SWF C (0.55) , then SCS (0.66), SWF B (0.77), and lastly SWF A (1.08). It is important to note that this analysis was performed on one of the replicates, the aspect ratios might look different for other replicates.

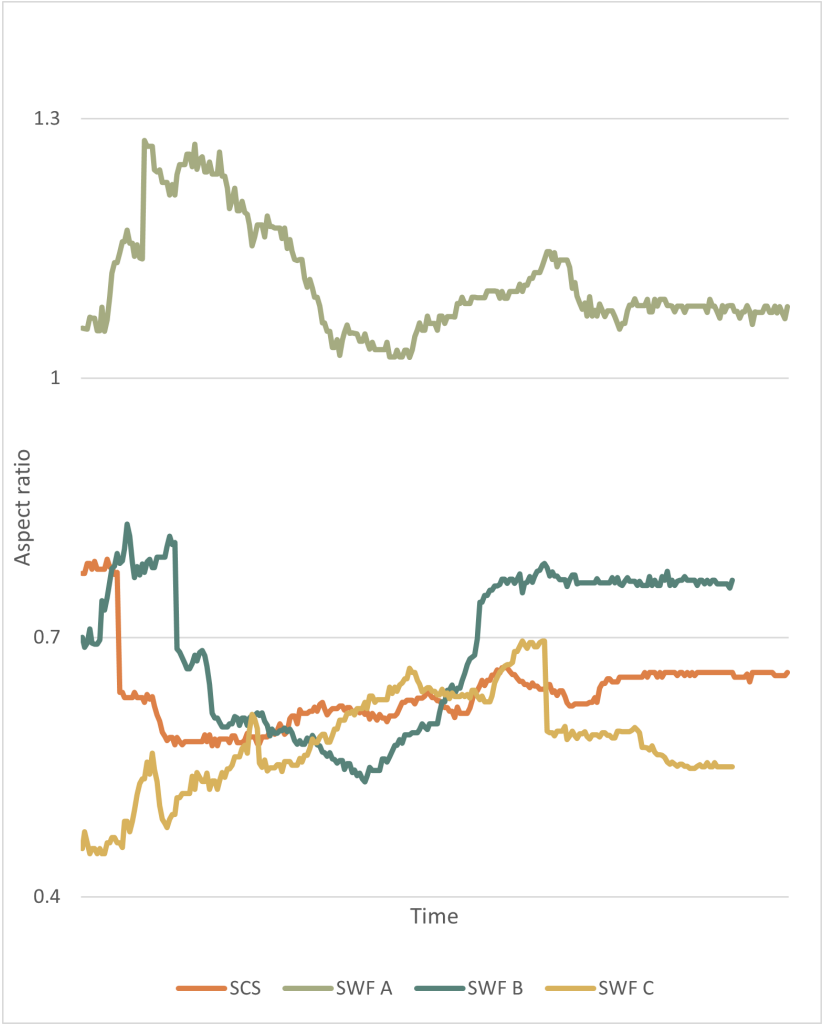

Figure 4.24: Aspect ratio as a function of time

The last method of pattern quantification used in this study included the comparison of the width and height of the fitted boxes. This method is somewhat similar to aspect ratio, but is another way of visualising the difference in spreading patterns. For uniform spreading patterns, there would be no difference between the width and the height (δ), however, if the spreading pattern elongates the difference would increase. Figure 4.25 displays that the δ was close to zero for SWF A, while for SCS, SWF C, and SWF B the height increased more than the width (larger δ). This indicates a more uniform spreading of SWF A, while the other fluids had a more elongated spreading pattern. As for the previous quantification methods, this analysis was performed on one of the replicates per fluid, the difference in width and height might look different for other replicates.

Figure 4.25: Width vs height as a function of time

5
Conclusions

Prior studies have shown that the spreading patterns of SCS and SWF A differed, as SCS was spread towards the bottom border of the dressing material as a result of gravitational forces, while SWF A spread more uniformely and did not reach the bottom border of the dressing. This study has confirmed the hypothises that the spreading pattern of the fluids depend on both capillary action and the aggregation of proteins in the dressing material.

SWF A had a higher surface tension than SCS, which resulted in a greater capillary action that counteracted gravitational forces to a greater extent than SCS. Alteration of the surface tension through the addition of surfactant (alkyl glucoside) resulted in a spreading behavior more similar to that of SCS.

Furthermore, the higher BSA content of SWF A compared to SCS resulted in more protein aggregation that seemed to create a solid protein barrier in the dressing material which prevented downwards flow of the test fluid. As the BSA content was altered to mimic that of SCS, less aggregation seemed to occur and a spreading behavior more similar to that of SCS was achieved.

This study also showed that both mass- and heat transfer processes are critical to visualise differences in spreading behavior between test fluids. The clinically relevant simulated wound model for chronic leg ulcers (FLUHTE) incorporates both processes and was the most useful test method to evaluate fluid-material interactions. The inclined plane method only included mass transfer processes and was useful to visualise transplanar wicking, but does not demonstrate the effects of fluid evaporation, which greatly effects protein aggregation. However, this method was still useful to study the spreading dynamics of test fluids.

A test fluid (SWF B) that mimics SCS in clinically relevant studies was achieved by optimising the composition of SWF A through altering the BSA content and addition of surfactant. Although, SWF B does have the same protein composition as SCS and further studies are needed to elucidate the impact of specific molecular weights on the functional properties and behavior of the test fluid. However, SWF B mimics the spreading behavior of SCS well enough to be a contestant for a new standardised test fluid that mimics the physico-chemical properties and spreading behavior of real chronic wound exudate.

5.1 Outlook

This study has shown that optimising the composition of SWF A by altering the BSA content and adding alkyl glucoside results in a test fluid (SWF B) that more closely mimics the physico-chemical properties and spreading behavior of real wound exudate and SCS. However, while SWF B have a similar BSA content to real wound exudate, it does not have an equivalent total protein content. From the results in this study, this does not seem to noticably effect the spreading behavior of the fluid, but the SDS-PAGE results showed that there were discrepencies in the protein composition between the SWFs and SCS. Further studies are needed to examine the influence of the protein composition of the fluid and to optimize the protein composition of SWF B in order to replicate the properties of SCS more effectively.

Spreading dynamics and pattern quantification has generated a lot of valuable information, however, the methodologies used in this study could be improved. For instance, the lighting conditions and camera settings when recording the timelapse of the spreading the dynamics could be optimised to generate higher quality images and more manageable data. Furthermore, the timelapse recorded in this study only captured the spreading dynamics that occured on the surface of the airlaid material. To gain a more comprehensive understanding of the spreading behavior of the fluid within the dressing material it would be valuable to record the spreading dynamics from a cross-sectional direction as well. Finally, the image analysis method used for pattern analysis could be improved upon to better quantify the spreading patterns of the fluids.

Bibliography

[1] C.K. Sen et al., "Human skin wounds: A major and snowballing threat to public health and the economy," *Wound Repair and Regeneration*, vol. 17, no. 6, pp. 763-862, Nov. 2009, doi: https://doi.org/10.1111/j.1524-475X.2009.00543.x

[2] K. Järbrink et al., "Prevalence and incidence of chronic wounds and related complications: a protocol for a systematic review", *Systematic reviews*, vol. 5, no. 152, Sep. 2016, doi: https://doi.org/10.1186/s13643-016-0329-y

[3] *Test methods for primary wound dressings*, EN 13726-1:2002, European Committee for Standardization, 2002. Available: https://www.en-standard.eu/bs-en-13726-1-2002-test-methods-for-primary-wound-dressings-aspects-of-absorbency/

[4] N.J. Trengove et al., "Biochemical analysis of wound fluid from nonhealing and healing chronic leg ulcers", *Wound Repair and Regeneration*, vol. 4, no. 2, Apr. 1996, doi: https://doi.org/10.1046/j.1524-475X.1996.40211.x

[5] S. Liu, S. Li, and J. Liu, "Jurin's law revisited: Exact meniscus shape and column height", *The European Physical Journal E*, vol. 41, no. 46, Mar. 2018, doi: https://doi.org/10.1140/epje/i2018-11648-1

[6] B. Cullen, and A. Gefen, "The biological and physiological impact of the performance of wound dressings", *International wound journal*, vol. 20, no. 4, pp. 1292-1303, Apr. 2023, doi: https://doi.org/10.1111/iwj.13960

[7] S. Ather, and K.G. Harding, "Wound management and dressings", in *Advanced Textiles for Wound Care*, 2nd ed., S.J. Tate, Ed., Cambridge, United Kingdom: Woodhead Publishing, 2019, ch. 1, pp. 1-22. [Online]. Available: https://www.sciencedirect.com/science/article/abs/pii/B9780081021927000011, Accessed on: 2023-01-26.

[8] V. Falanga, "Wound healing and its impairment in the diabetic foot", *The Lancet*, vol. 366, no. 9498, pp. 1736-1743, Nov. 2005, doi: https://doi.org/10.1016/S0140-6736(05)67700-8

[9] S. Guo, and L.A. DiPietro, "Factors Affecting Wound Healing", *Journal of Dental Research*, vol. 89, no. 3, pp. 219-229, Mar. 2010, doi: https://doi.org/10.1177/0022034509359125

[10] A.J. Singer, and R.A Clark, "Cutaneous wound healing", *The New England journal of medicine*, vol. 341, no. 10, pp. 738-746, Sep. 1999, doi: https://doi.org/10.1056/NEJM199909023411006

[11] M. Leveriza-Oh, T.J. Phillips, "Dressings and Postoperative Care", in *Surgery of the Skin*, 1st ed., J.K Robinson et al., Ed. Maryland Heights, USA: Mosby, 2005, ch. 8, pp. 117-135. [Online]. Available: https://www.sciencedirect.com/science/article/abs/pii/B9780323027526500134, Accessed on: 2023-01-26

[12] G. Power et al., "Measurement of pH, exudate composition and temperature in wound healing: a systematic review", *Journal of wound care*, vol. 26, no. 7, pp. 381-397, Jul. 2017, doi: https://doi.org/10.12968/jowc.2017.26.7.381

[13] M. Werthén, "Wound exudate composition - A literature update on the composition of wound exudate from acute and hard-to-heal wounds", Sahlgrenska Academy, University of Gothenburg, Gothenburg, Sweden, 2018.

[14] K.F. Cutting, "Wound exudate: composition and functions", *British journal of community nursing*, vol. 8, no. 3, pp. 4-9, Sep. 2013, doi: https://doi.org/10.12968/bjcn.2003.8.Sup3.11577

[15] Expert working group. and Satellite expert working group., "Wound exudate and the role of dressings. A consensus document", *International wound journal*, vol. 5, no. 1, 2007, doi: https://doi.org/10.1111/j.1742-481X.2008.00439.x

[16] U. Adderley, "Wound exudate: what it is and how to manage it", *Wound Essentials*, vol. 3, pp. 8-13, 2008.

[17] K. Harding et al., "WUWHS Consensus Document: Wound exudate, effective assessment and management", *Wounds Internatioinal*, Feb. 2019, URL: https://woundsinternational.com/consensus-documents/wuwhs-consensus-document-wound-exudate-effective-assessment-and-management-2/

[18] J. Bianchi, "The effective management of exudate in chronic wounds", *Wounds International*, Vol. 3, No. 4, pp. 14-16, Dec. 2012, URL: https://woundsinternational.com/journal-articles/the-effective-management-of-exudate-in-chronic-wounds/

[19] Britannica, The Editors of Encyclopaedia. "Protein summary", in *Encyclopaedia Britannica*. USA: Encyclopaedia Britannica Inc., 2021. [Online]. Available: https://www.britannica.com/summary/protein. Accessed on: 2023.04.18

[20] E. Buxbaum, *Fundamentals of Protein Structure and Function*. 2nd ed., Switzerland: Springer International Publishing, 2015.

[21] L.G. Phillips, D.M. Whitehead, and J. Kinsella, *Structure-Function Properties of Food Proteins*. 1st ed., Cambridge, USA: Academic Press, 1994

[22] H.S. Stoker, *Feneral, Organic, and Biological Chemistry*. 7th ed., Boston, USA: Cengage Learning, 2015

[23] Britannica, The Editors of Encyclopaedia. "Denaturation", in *Encyclopaedia Britannica*. USA: Encyclopaedia Britannica Inc., 2021. [Online]. Available: https://www.britannica.com/science/denaturation. Accessed on: 2023.04.18

[24] A. Schön et al., "Denatured state aggregation parameters derived from concentration dependence of protein stability", *Analytical biochemistry*, Vol. 488, pp. 45-50, Nov. 2015, doi: https://doi.org/10.1016/j.ab.2015.07.013

[25] A.J. Weids, S. Ibstedt, M.J. Tamás, and C.H. Grant, "Distinct stress conditions result in aggregation of proteins with similar properties", *Scientific Reports*, Vol 6, No. 24554, Apr. 2016, doi: https://doi.org/10.1038/srep24554

[26] G. Merlini et al., "Protein Aggregation", *De Gruyter*, Vol. 39, No. 11, pp. 1065-1075, Jun. 2005, doi: https://doi.org/10.1515/CCLM.2001.172

[27] M.J. Treuheit, A.A. Kosky, and D.N. Brems, "Inverse relationship of protein concentration and aggregation", *Pharmaceutical Research*, Vol. 19, No. 4, pp. 511-516, Apr. 2002, doi: https://doi.org/10.1023/a:1015108115452

[28] A.M. Hyde et al., "General Principles and Strategies for Salting-Out Informed by the Hofmeister Series", *Organic Process Research & Development*, Vol. 21, No. 9, pp. 1355-1370, Aug. 2017, doi: https://doi.org/10.1021/acs.oprd.7b00197

[29] Svensby, A., Craig, M., Gergely, AB., Ronkvist, Å., "Influence of test fluid composition on the evaluation of Fluid Handling Capacity of wound dressings". Poster presentation, Mölnlycke Health Care.

[30] L. Lins, and R. Brasseur, "The hydrophobic effect in protein folding", *FASEB journal: official publication of the Federation of American Societies for Experimental Biology*, Vol. 9, No. 7, pp. 535-540, Apr. 1995, doi: https://doi.org/10.1096/fasebj.9.7.7737462

[31] M.A. Woldeyes et al., "Temperature Dependence of Protein Solution Viscosity and Protein-Protein Interactions: Insights into the Origins of High-Viscosity Protein Solutions", *Molecular pharmaceutics*, Vol. 17, No. 12, pp. 4473-4482, Dec. 2020, doi: https://doi.org/10.1021/acs.molpharmaceut.0c00552

[32] M. Aguirre-Ramírez, H. Silva-Jiménez, I.M. Banat, M.A. Díaz De Rienzo, "Surfactants: physicochemical interactions with biological macromolecules", *Biotechnology Letters*, Vol. 43, pp. 523-535, Feb. 2021, doi: https://doi.org/10.1007/s10529-020-03054-1

[33] S. Hasatstri et al., "Comparison of the Morphological and Physical Properties of Different Absorbent Wound Dressings", *Dermatology research and practice*, Vol. 2018, May. 2018, doi: https://doi.org/10.1155/2018/9367034

[34] H. Begum, T. Tanni, and M. Shahid, "Analysis of Water Absorption of Different Natural Fibers, *Journal of Textile Science and Technology*, Vol. 7, pp. 152-160, Nov. 2021, doi: https://doi.org/10.4236/jtst.2021.74013

[35] J.W. Gooch, "Super Absorbent Fibers", in *Encyclopedic Dictionary of Polymers*, 2nd ed., J.W. Gooch, Ed. New York, USA: Springer, 2011, pp. 712-714. [Online]. Available: https://link.springer.com/referenceworkentry/10.1007/978-1-4419-6247-8_11416, Accessed on: 2023-04-24

[36] Mölnlycke Health Care AB, "Mepilex Border Flex", 2018. [Online]. Available: https://www.molnlycke.se/produkter-losningar/mepilex-border-flex/. (accessed on: 2023-04-24)

[37] A. Sood, M.S. Granick, and N.L. Tomaselli, "Wound Dressings and Comparative Effectiveness Data", *Advances in wound care*, Vol 3, No. 8, pp. 511-529, Aug. 2014, doi: https://doi.org/10.1089/wound.2012.0401

[38] B. Das, A. Das, V.K. Kothari, R. Fangueiro, and M. de Araujo, "Moisture transmission through textiles: Part I: Processes involved in moisture transmission and the factors at play", *Autex Research Journal*, Vol. 7, No. 2, pp. 100-110, Jun. 2007, url: https://www.researchgate.net/publication/279571256_Moisture_transmission_through_textiles_Part_I_Processes_involved_in_moisture_transmission_and_the_factors_at_play

[39] Y. Li, Q. Zhu, "Simultaneous Heat and Moisture Transfer with Moisture Sorption, Condensation, and Capillary Liquid Diffusion in Porous Textiles", *Textile Research Journal*, Vol. 73, No. 6, pp. 515-524, Jun. 2003, doi: https://doi.org/10.1177/004051750307300609

[40] L. Yang, "Superabsorbent Fibers for Comfortable Disposable Medical Protective Clothing", *Advanced Fiber Materials*, Vol. 2, No. 3, pp. 140-149, Jun. 2020, doi: https://doi.org/10.1007/s42765-020-00044-w

[41] A. Patnaik, R.S. Rengasamy, V.K. Kothari, and A. Ghosh, "Wetting and Wicking in Fibrous Materials", *Textile Progress*, Vol. 38, No. 1, pp. 1-105, doi: https://doi.org/10.1533/jotp.2006.38.1.1

[42] K.Y. Law, "Definitions for Hydrophilicity, Hydrophobicity, and Superhydrophobicity: Getting the Basics Right", *The Journal of Physical Chemistry Letters*, Vol. 5, No. 4, pp. 686-688, Feb. 2014, doi: https://doi.org/10.1021/jz402762h

[43] R. Masoodi, K.M. Pillai, *Wicking in Porous Materials: Traditional and Modern Modeling Approaches*, Vol. 1, Boca Raton, FL, USA: Taylor Francis, 2013. [Online]. Available: https://books.google.se/books/about/Wicking_in_Porous_Materials.html?id=0gHSBQAAQBAJ&redir_esc=y, Accessed on: 2023-05-03

[44] J. Cottet, P. Renaud, "Introduction to microfluidics", in *Developments in Biomedical Engineering and Bioelectronics*, E. Chappel, Ed. Cambridge, USA: Academic Press, 2020, ch. 1, pp. 3-17. [Online]. Available: https://www.sciencedirect.com/science/article/pii/B9780128198384000146, Accessed on: 2023.05.03

[45] Y.L. Hsieh, "Liquid Transport in Fabric Structures", *Textile Research Journal*, Vol. 65, No. 5, pp. 299-307, May. 1995, doi: http://doi.org/10.1177/004051759506500508

[46] L. Maduna, and A. Patnaik, "Heat, moisture and air transport through clothing textiles", *Textile Progress*, Vol. 52, No. 3, pp. 129-166, Sep. 2021, doi: https://doi.org/10.1080/00405167.2021.1955524

[47] R. Xu et al., "Controlled water vapor transmission rate promotes wound-healing via wound re-epithelialization and contraction enhancement", *Scientific Reports*, Vol. 6, No. 24596, Apr. 2016, doi: https://doi.org/10.1038/srep24596

[48] T. Arakawa, D. Ejima, and T. Akuta, "Protein aggregation under high concentration/density state during chromatographic and ultrafiltration processes", *International Journal of Biological Macromolecules*, Vol. 95, pp. 1153-1158, Feb. 2017, doi: https://doi.org/10.1016/j.ijbiomac.2016.11.005

Department of Chemistry and Chemical Engineering
CHALMERS UNIVERSITY OF TECHNOLOGY
Gothenburg, Sweden 2023
www.chalmers.se

CHALMERS
UNIVERSITY OF TECHNOLOGY